PERSISTENT HOMOLOGY METHOD OF ROAD NETWORK CONNECTIVITY CONDITIONED BY WATERWAY PROXIMITY FOR FLOOD MANAGEMENT IN BANGKOK

NALINPAT PONOI

AN INDEPENDENT STUDY SUBMITTED IN PARTIAL FULFILLMENT OF THE
REQUIREMENT FOR THE DEGREE OF MASTER OF SCIENCE IN DATA SCIENCE AND ANALYTICS
KMITL DIGITAL ANALYTICS AND INTERLLIGENCE CENTER SCHOOL OF SCIENCE
KING MONGKUT'S INSTITUTE OF TECHNOLOGY LADKRABANG
2025

KMITL-2025-SC-M-017-035

Independent Study Title	Persistent Homology Method of Road Network Connectivity Conditioned by Waterway Proximity for Flood Management in Bangkok
Student Name	Nalinpat Ponoi
Student ID	66056045
Degree	Master of Science (Data Science and Analytics) KMITL Digital Analytics and Intelligence Center
Year	2025
Independent Study Advisor	Asst.Prof.Dr. Jiraphat Yokrattanasak

Abstract

This study explores the topological structure of Bangkok's road network relative to its waterway system using persistent homology to inform flood management strategies. Utilizing OpenStreetMap data, we derived two filtrations based on the distance from road segments to the nearest waterway: one using direct distance and the other using an inversely related measure. The persistent homology analysis revealed distinct connectivity patterns under each filtration, visualized through barcodes, diagrams, and Betti plots. Key thresholds indicating significant topological changes were identified. We discuss the potential application of these findings for identifying flood susceptibility, suggesting potentially safer routes, and informing data-driven flood trigger levels based on critical topological thresholds.

Keywords : Flood Management, Road Network, Topology, Persistent Homology

Acknowledgment

I would like to express my sincere gratitude to those who have supported me throughout this work. My special thanks go to my supervisor, Asst.Prof.Dr. Jiraphat Yokrattanasak, for their invaluable guidance and support. I am also deeply thankful for the encouragement of my friends and the unwavering support of my family during this period.

Nalinpat Ponoi

Content

List of Figures

List of Figures (Continue)

Figure **Page**

Chapter 1

Introduction

1.1 Introduction

Urban flooding presents significant and growing challenges to infrastructure, public safety, and economic stability, particularly in densely populated, low-lying metropolitan areas such as Bangkok. The vulnerability of the city is exacerbated by factors that include its geographical location, rapid urbanization in recent decades, and the consequent alteration of natural drainage systems (Nair et al. 2014). While advanced flood forecasting and management systems incorporating real-time data and machine learning are being developed for Bangkok, there remains a need for complementary approaches to understand and predict flood risk, especially those leveraging the structural properties of urban infrastructure networks. Effective identification of flood-prone zones is crucial for proactive mitigation strategies and efficient emergency response plans.

In recent years, Topological Data Analysis (TDA) has emerged as a powerful suite of tools for extracting robust, global structural information from large and complex datasets. Persistent homology, a central technique within TDA, excels at identifying and quantifying topological features (like connected components and cycles) across different scales, providing insights into the intrinsic shape and connectivity of data. Its proven ability to analyze spatial data, identify void regions, and track features across scales makes it particularly well-suited for analyzing complex network structures inherent in urban environments and geographical information science (GIS) applications (Corcoran et al. 2023).

Predicting flood susceptibility is inherently complex, with established research demonstrating the importance of analyzing numerous interacting geo-environmental factors. As highlighted in the literature Mosiva et al. 2018, Rahmati et al. 2015, Tehrany et al. 2014 and Zhao et al. 2018, variables such as elevation, slope, land use/land cover (LULC), soil type, rainfall patterns, and, crucially, *distance to waterways* are commonly employed inputs in flood modeling and susceptibility mapping. While acknowledging the combined influence of these diverse elements, the present study adopts a focused approach by isolating the distance to the nearest waterway as the primary parameter. This allows for a targeted investigation, using persistent homology, into the specific relationship between the topological structure of Bangkok's road network and its proximity to water features, serving as a foundational analysis within this multifaceted domain.

Concurrently, openly accessible geospatial datasets like OpenStreetMap (OSM) offer unprecedented opportunities for urban analysis and risk assessment. OSM provides detailed, community-sourced data on various features, including extensive road networks and waterway systems. This study investigates the application of persistent homology to predict flood-prone roads in Bangkok, leveraging network data extracted from OpenStreetMap. We propose an approach where the flood risk associated with road segments is initially scored based on their proximity to waterways – a primary factor contributing to inundation risk. By analyzing the topological characteristics derived from the spatial relationships between the road network and waterway network using persistent homology, we aim to identify roads that are structurally vulnerable to flooding based on this proximity scoring.

The outcomes of this research offer significant practical implications for Bangkok's ongoing flood management efforts. Identifying high-risk road segments can directly inform urban planning and disaster management, aiding in the optimization of evacuation routes during flood events, facilitating the targeted delivery of essential supplies such as food and medicine to affected areas, and guiding long-term infrastructure planning, potentially including the strategic placement of new artificial waterways or flood defenses, complementing existing top-down engineering approaches.

Furthermore, this work serves as a foundational step with potential for considerable expansion. Future research could enhance the prediction model by incorporating additional risk factors. These might include relative elevation differences between roads and adjacent waterways, absolute elevation above mean sea level, historical inundation patterns recorded potentially via OSM or other sources, or land use characteristics, potentially integrating these variables into a more comprehensive, multi-factor risk assessment framework using TDA methodologies.

1.2 Research Objectives

1. To investigate and apply persistent homology as a novel analytical tool for understanding the structural relationship between road and waterway networks relevant to flood susceptibility.

2. To develop a method for scoring flood susceptibility for road segments based fundamentally on their spatial proximity to waterways.

1.3 Scope of Study

1. Geographical Area: The study focuses exclusively on the area of Bangkok, Thailand.

2. Data Sources: The analysis relies solely on the road network within the keys `highway=trunk, primary, secondary, tertiary, unclassified` and the waterway network within the keys `waterway=river, canal, drain, ditch`,

with data acquired from OpenStreetMap (OSM). Other potential data sources (e.g., detailed hydrological data, specific infrastructure capacity) are not incorporated.

3. Analysis Basis: The insights aimed at decision support in this study are primarily derived using a single factor: the spatial proximity of road segments to waterways. This proximity measure serves as the key parameter for the topological analysis performed. Other contributing factors acknowledged in the introduction (e.g., elevation relative to waterways or sea level, historical flood data, rainfall patterns, soil type, drainage capacity) are explicitly outside the scope of this specific investigation but noted as avenues for future work.

4. Methodology: The core analytical technique employed is persistent homology, a method from Topological Data Analysis (TDA). While acknowledging other flood prediction methods exist, this study concentrates on evaluating the utility of TDA in this context.

1.4 Contribution to knowledge

1. To obtain a new decision-support approach conditioned by waterway proximity for flood management on the road network of Bangkok.

2. To obtain a prototype for analyzing road data using a TDA-based framework that offers planners a structural and multi-scale network perspective.

3. To inform flood management decisions based on the analysis results.

1.5 Methodology Overview

1. Data Acquisition and Preprocessing: Obtain road network and waterway network data for Bangkok from OpenStreetMap. Preprocess the data to ensure it is suitable for network and topological analysis (e.g., cleaning, formatting, ensuring connectivity).

2. Proximity Calculation: Calculate the spatial proximity (distance) between each road segment and the nearest waterway feature. This distance value serves as the primary parameter for the subsequent topological analysis.

3. Topological Analysis: Apply persistent homology (H_0) techniques to the road network data. This involves analyzing the evolution of topological features (connected components) by defining graph filtrations based directly on the calculated waterway proximity parameter.

4. Interpretation for Decision Support: Interpret the persistent homology outputs (e.g., persistence diagrams, barcodes) to identify significant topological features (e.g., highly persistent components, critical thresholds). Analyze how these features relate to waterway proximity, providing insights into the network's structural connectivity patterns relevant for informing flood management decisions and identifying areas for further investigation.

Chapter 2

Literature Review

This section provides a background on the key concepts and data sources underpinning this research: the mathematical foundations of homology theory, the methodology of persistent homology, and the nature of OpenStreetMap data used in the analysis.

In recent years, Topological Data Analysis (TDA) has emerged as a powerful mathematical framework for analyzing the *shape* and structure of complex, high-dimensional data. TDA focuses on identifying robust, global features that are invariant under continuous deformations, providing insights that complement traditional geometric and statistical methods. A cornerstone of TDA is *Persistent Homology* (PH), a computational technique that quantifies topological features—such as connected components, loops (tunnels), and voids (cavities)—across multiple spatial or parametric scales. By tracking when these features appear (birth) and disappear (death) as a resolution parameter changes, PH identifies features that *persist* over a significant range of scales, distinguishing potentially meaningful structures from noise or sampling artifacts. This multiscale approach provides a robust and compact representation of the data's qualitative features. PH has found increasing application in various scientific domains, including neuroscience, materials science, and notably, computational biology for analyzing biomolecular structures and dynamics. For more details, see Aktas et al. (2019).

The computation of persistent homology fundamentally relies on the construction of a filtration. A *filtration* is a sequence of nested topological spaces, typically simplicial complexes, indexed by a continuously increasing parameter (e.g., distance, time, density, or interaction strength). This sequence models the evolution of the data's structure as the parameter varies. The specific choice of filtration is critical, as it determines which aspects of the data's structure are being probed and, consequently, what topological features are captured by the resulting persistent homology. Different filtrations applied to the same underlying data can yield different topological summaries, reflecting distinct structural perspectives.

2.1 Simplicial Complexes and Homology

Homology theory is a fundamental branch of algebraic topology that associates algebraic structures, typically abelian groups, to topological spaces to study their connectivity properties. The framework often begins with the concept of a simplicial complex, which provides a combinatorial way to represent shapes. We briefly state some important mathematical tools here. For more details, see Herbert 2014,

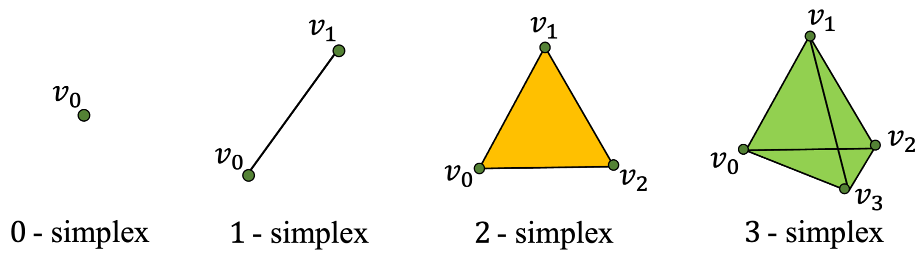

Figure 2.1 Examples of simplex in each dimension.

Hatcher 2002, and Munkres 1984.

A **graph** $G = (V, E)$ consists of a set of vertices V (nodes) and a set of edges E, where each edge connects a pair of vertices. Graphs represent pairwise relationships and form the basis for 1-dimensional simplicial complexes.

Definition 2.1.1. A **k-simplex** is the convex hull of $k + 1$ affinely independent points in a Euclidean space. Combinatorially, it can be thought of as a set of $k+1$ vertices. A **face** of a simplex is the convex hull of any non-empty subset of its defining vertices.

For examples,

- A 0-simplex $[v_0]$ is a vertex.
- A 1-simplex $[v_0, v_1]$ is an edge connecting vertices v_0 and v_1.
- A 2-simplex $[v_0, v_1, v_2]$ is a triangle with its interior.
- A 3-simplex $[v_0, v_1, v_2, v_3]$ is a tetrahedron with its interior.

See Figure 2.1 for the visualization.

Definition 2.1.2. A **simplicial complex** K is a finite collection of simplices such that:

1. (Face Property) If a simplex σ is in K, then all faces of σ are also in K.
2. (Intersection Property) If $\sigma_1, \sigma_2 \in K$, then their intersection $\sigma_1 \cap \sigma_2$ is either empty or a face of both σ_1 and σ_2.

For examples of a simplicial complex and a configuration that is not a simplicial complex, see Figure 2.2 and Figure 2.3, respectively.

To analyze the structure of a simplicial complex K, we define **chain groups**.

Definition 2.1.3. A k-chain is a formal sum of oriented k-simplices of K. The k-th chain group, denoted $C_k(K)$, is the free abelian group generated by the set of oriented k-simplices in K.

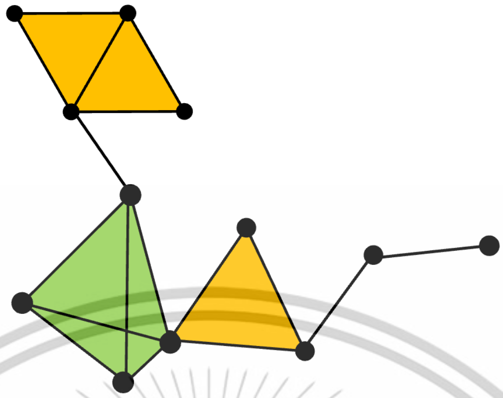

Figure 2.2 An example of a simplicial complex. The non-empty intersection of any two simplices of K is a face of each of them.

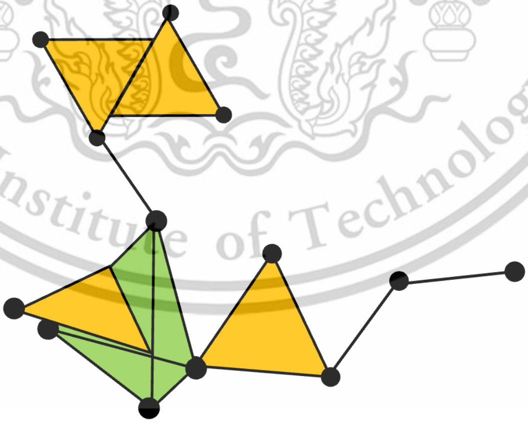

Figure 2.3 An example of a configuration that is not a simplicial complex. This is because there are non-empty intersections of two simplices within the complex that are not faces of any simplex.

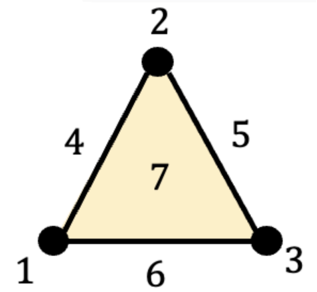

Figure 2.4 Triangle 7 has edges 4, 5, and 6 as its boundary, so $\partial(7) = 4+5+6$. Edge 4 has vertices 1 and 2 as its boundary, thus $\partial(4) = 1+2$. Similarly, $\partial(5) = 2+3$ and $\partial(6) = 3+1$. Since we are working in $\mathbb{Z}_2$, it follows that $\partial(\partial(7)) = \partial(4+5+6) = \partial(4) + \partial(5) + \partial(6) = (1+2) + (2+3) + (3+1) = 0$.

Coefficients are often taken in $\mathbb{Z}$ (integers) or $\mathbb{Z}_2$ (integers modulo 2), the latter simplifying calculations by ignoring orientation issues.

In this work, we use the space $\mathbb{Z}_2$ to be coefficients, that is

$$C_k(K) = \{\sum_i a_i \sigma_i \mid \sigma_i \text{ is a } k\text{-simplex in } K, a_i \in \mathbb{Z}_2\}.$$

Definition 2.1.4. The **boundary map** $\partial_k : C_k(K) \to C_{k-1}(K)$ is a homomorphism defined for an oriented k-simplex $\sigma = [v_0, v_1, \ldots, v_k]$ as: $\partial_k(\sigma) = \sum_{i=0}^{k} (-1)^i [v_0, \ldots, \hat{v}_i, \ldots, v_k]$ where $[v_0, \ldots, \hat{v}_i, \ldots, v_k]$ denotes the $(k-1)$-simplex obtained by removing the vertex v_i.

The boundary map extends linearly to all k-chains. A fundamental property of the boundary map is that the boundary of a boundary is zero. See, Figure 2.4 as an example.

Proposition 2.1.5. *For integer $k \geq 1$, $\partial_{k-1} \circ \partial_k = 0$.*

Proof. For $k = 1$, $\partial_0 = 0$, the proof is done. Next, assume that $k \geq 2$. Since ∂_{k-1} is a homomorphism, we can write:

$$\begin{aligned}
\partial_{k-1}(\partial_k(\sigma)) &= \partial_{k-1}\left(\sum_{j=0}^{k}(-1)^j[v_0,\ldots,\hat{v}_j,\ldots,v_k]\right) \\
&= \sum_{j=0}^{k}(-1)^j\partial_{k-1}([v_0,\ldots,\hat{v}_j,\ldots,v_k]) \\
&= \sum_{j=0}^{k}(-1)^j(\sum_{i=0}^{j-1}(-1)^i[v_0,\ldots,\hat{v}_i,\ldots,\hat{v}_j,\ldots,v_k] \\
&\quad + \sum_{i=j+1}^{k}(-1)^{i-1}[v_0,\ldots,\hat{v}_j,\ldots,\hat{v}_i,\ldots,v_k]) \\
&= \sum_{j=0}^{k}\sum_{i=0}^{j-1}(-1)^{j+i}[v_0,\ldots,\hat{v}_i,\ldots,\hat{v}_j,\ldots,v_k] \\
&\quad + \sum_{j=0}^{k}\sum_{i=j+1}^{k}(-1)^{j+i-1}[v_0,\ldots,\hat{v}_j,\ldots,\hat{v}_i,\ldots,v_k]
\end{aligned}$$

Since $k \geq 2$, the $(k-2)$-simplices are well-defined (i.e., dimension ≥ 0). Every $(k-2)$-simplex obtained by removing two vertices from σ appears exactly twice in the sum, with opposite signs. Therefore, all terms cancel out, and we have:

$$\partial_{k-1}(\partial_k(\sigma)) = 0$$

□

Definition 2.1.6. The group of k**-cycles**, $Z_k(K)$, consists of k-chains with zero boundary

$$Z_k(K) = \ker \partial_k = \{c \in C_k(K) \mid \partial_k(c) = 0\}.$$

Definition 2.1.7. The group of k**-boundaries**, $B_k(K)$, consists of k-chains that are boundaries of $(k+1)$-chains

$$B_k(K) = \operatorname{im} \partial_{k+1} = \{\partial_{k+1}(d) \mid d \in C_{k+1}(K)\}.$$

Since $\partial \circ \partial = 0$, every boundary is a cycle, so $B_k(K)$ is a subgroup of $Z_k(K)$.

Definition 2.1.8. The k**-th homology group** $H_k(K)$ is defined as the quotient group

$$H_k(K) = Z_k(K)/B_k(K).$$

The homology group $H_k(K)$ captures information about the k-dimensional holes in the topological space represented by K. Let β_i be the number of classes in $H_i(K)$.

1. β_0 measures the number of connected components.

2. β_1 measures the number of independent loops or tunnels.

3. β_2 measures the number of enclosed voids or cavities.
And so on for higher dimensions.

2.2 Persistent Homology

While classical homology provides topological invariants for a single space, persistent homology extends this analysis to study how topology changes across a sequence of spaces, typically arising from data. This is achieved through the concept of a filtration. The choice of filtration dictates how the topological space evolves and which structural aspects of the data are emphasized.

A **filtration** of a simplicial complex K is a nested sequence of subcomplexes, indexed by a parameter:

$$\emptyset = K_0 \subseteq K_1 \subseteq K_2 \subseteq \cdots \subseteq K_m = K$$

Filtrations can be constructed in various ways depending on the input data. In this work, we use a *clique complex filtration*.

2.2.1 Clique Complex Filtration

Given an undirected graph $G = (V, E)$, its **clique complex**, often denoted $K(G)$ or $Cl(G)$ (and sometimes referred to as the flag complex), is a specific type of abstract simplicial complex constructed directly from the graph's structure. The construction proceeds as follows:

1. Vertices (0-simplices): The set of vertices of the simplicial complex $K(G)$ is identical to the set of vertices V of the graph G. Each vertex in the graph corresponds to a 0-simplex in the complex.

2. Higher-dimensional Simplices: For any integer $k \geq 1$, a set of $k+1$ distinct vertices $v_0, v_1, \ldots, v_k \subseteq V$ forms a k-simplex in $K(G)$ if and only if these $k+1$ vertices constitute a (k+1)-clique in the graph G. Recall that a $(k+1)$-clique is a subgraph where every pair of distinct vertices in the set $v_0, v_1, \ldots, v_k$ is connected by an edge in E.

A 1-simplex $[v_i, v_j]$ exists in $K(G)$ if and only if the edge (v_i, v_j) exists in E (i.e., 1-simplices correspond to edges, which are 2-cliques). A 2-simplex $[v_i, v_j, v_l]$ exists in $K(G)$ if and only if the vertices v_i, v_j, v_l form a triangle in G (i.e., edges (v_i, v_j), (v_j, v_l), and (v_i, v_l) all exist in E; this is a 3-clique). A 3-simplex $[v_i, v_j, v_l, v_m]$ exists in $K(G)$ if and only if the four vertices form a tetrahedron in G (a 4-clique), and so on. This construction guarantees that $K(G)$ is a valid simplicial complex. This is because the defining properties of a simplicial complex are automatically satisfied:

- Face Property: Every face of a simplex in $K(G)$ is also a simplex in $K(G)$. If $v_0, \ldots, v_k$ forms a k-simplex (i.e., a $(k+1)$-clique), then any subset of these vertices also forms a clique, and thus corresponds to a lower-dimensional simplex (a face) which is included in $K(G)$.

- Intersection Property: The intersection of any two simplices in $K(G)$ is either empty or a face of both. If two simplices correspond to cliques C_1 and C_2, their intersection corresponds to the subgraph induced by $V(C_1) \cap V(C_2)$. Since the intersection of two cliques is always a clique (possibly empty), the intersection corresponds to a simplex that is a face of both original simplices.

The clique complex $K(G)$ therefore provides a canonical way to lift the structure of a graph G into a higher-dimensional topological space. It encodes all higher-order connectivity patterns that can be inferred solely from the pairwise connections (edges) present in the graph, under the assumption that if all pairwise connections within a set of vertices exist, then the corresponding higher-order interaction (simplex) also exists.

Let $\{G_\epsilon \mid \epsilon \in I\}$ be a sequence of graphs indexed by a parameter ϵ from a totally ordered set I. Assume this sequence is generated such that it forms a nested sequence, meaning that for any $\epsilon_i, \epsilon_j \in I$ with $\epsilon_i \leq \epsilon_j$, we have $G_{\epsilon_i} \subseteq G_{\epsilon_j}$ (as subgraphs). This is typically achieved by starting with a base graph G (often weighted) and defining G_ϵ based on a threshold or condition related to ϵ.

For each graph $G_\epsilon = (V_\epsilon, E_\epsilon)$ in the sequence, its clique complex (or flag complex), denoted $K(G_\epsilon)$, is the abstract simplicial complex whose vertex set is V_ϵ, and whose k-simplices (for $k \geq 0$) are precisely the subsets $v_0, v_1, \ldots, v_k \subseteq V_\epsilon$ that form a $(k+1)$-clique in G_ϵ.

The **clique complex filtration** associated with the nested graph sequence G_ϵ is the sequence of simplicial complexes $\{K(G_\epsilon) \mid \epsilon \in I\}$, ordered according to the parameter ϵ. Due to the nesting of the graphs ($G_{\epsilon_i} \subseteq G_{\epsilon_j}$) and the nature of the clique complex construction, this sequence of complexes is also nested:

$$K(G_{\epsilon_i}) \subseteq K(G_{\epsilon_j}) \quad \text{for all } \epsilon_i, \epsilon_j \in I \text{ with } \epsilon_i \leq \epsilon_j$$

This nested sequence $K(G_\epsilon)$ constitutes the clique complex filtration.

2.2.2 Persistent Homology

Persistent homology tracks the evolution of homology classes (representing topological features) throughout this sequence. It identifies when features (e.g., connected components, loops, voids) appear and when they disappear or merge with older features. See Figure 2.5 as an example.

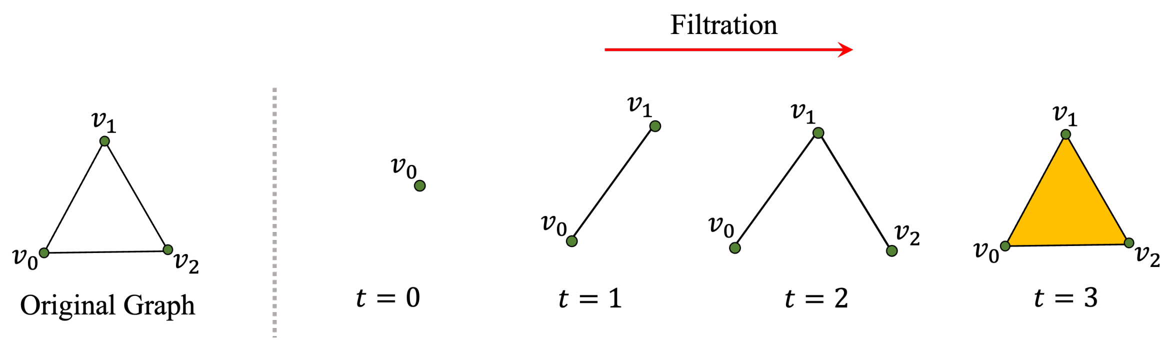

Figure 2.5 An example of a clique complex filtration derived from a graph. Simplices are added to the corresponding clique complex as the filtration parameter increases according to the filtration rule (e.g., thresholding edge weights). Notably, whenever a set of vertices forms a clique (complete subgraph) in the graph at a certain parameter value, the corresponding higher-dimensional simplex (representing its *filled interior*) is immediately included in the clique complex.

For $i \leq j$, K_i is a subcomplex of K_j, which can be written as an inclusion map $f^{i,j} : K_i \hookrightarrow K_j$. For the set of p-cycles, $f_p^{i,j} : Z_p(K_i) \hookrightarrow Z_p(K_j)$. This induces a map on homology

$$\varphi_p^{i,j} : H_p(K_i) \rightarrow H_p(K_j),$$

which generally is not an inclusion map. Let γ be a class in $H_p(K_i)$ and $z \in Z_p(K_i)$ a representative cycle. Let $\varphi_p^{i,j}(\gamma)$ be the class in $H_p(K_j)$ that contains $f_p^{i,j}(z)$. It takes a p-cycle in K_i and pushes forward to K_j. The image of $\varphi_p^{i,j}$ is called a **persistent homology group**.

The **birth time** b of a homology class is the index i (or parameter value ϵ_i) of the first complex K_i in the filtration where the class appears. The **death time** d is the index j ($j > i$) where the class merges into an older class (one born earlier) or becomes trivial within $H_k(K_j)$. The **persistence** of the feature is the interval $[b, d)$. Features that exist in the final complex K_m are often assigned a death time of $d = \infty$.

The results of persistent homology are commonly visualized in two ways:

- **Persistence Barcode**: Each homology class with birth time b and death time d is represented by a horizontal bar (line segment) $[b, d)$. The collection of all such bars for dimension k forms the k-th persistence barcode. Long bars correspond to features that persist across a wide range of scales and are often considered significant topological signatures of the data. Short bars are often interpreted as noise.

- **Persistence Diagram**: Each class with lifetime $[b, d)$ is plotted as a point (b, d) in the 2D plane. All points lie above the diagonal line $y = x$. Points far from the diagonal represent persistent features, while points close to the diagonal represent features with short lifetimes (topological noise).

Persistent homology provides a multi-scale summary of the topology of data and is robust to small perturbations. Foundational work and comprehensive introductions can be found in Edelsbrunner (2010).

2.3 OpenStreetMap Data in Topological Analysis

OpenStreetMap (OSM) is a global collaborative project that creates and distributes free, editable geographic data (OpenStreetMap contributors). It operates on the principle of Volunteered Geographic Information (VGI), where users contribute and maintain data about roads, buildings, land use, waterways, and points of interest. Its open nature makes it an increasingly valuable resource for research and applications requiring detailed geospatial information, including urban planning and disaster management.

Within OSM, infrastructure relevant to this study includes:

- **Street Network**: OSM contains highly detailed data representing roads, highways, streets, footpaths, etc., typically as sequences of connected nodes (vertices) forming lines (edges). Associated attributes can include road type (e.g., motorway, residential), surface, number of lanes, and names. This constitutes a complex graph embedded in geographic space.

- **Waterways**: Similarly, OSM maps natural and artificial waterways such as rivers, canals, streams, and drains. These are also represented geometrically as lines or polygons, forming another crucial network layer for hydrological and flood-related studies.

The network structures inherent in OSM data lend themselves naturally to analysis using graph theory and TDA. Representing street and waterway networks as graphs or simplicial complexes allows the application of homology and persistent homology to study their topological properties. Recent work highlights the potential of TDA, including persistent homology, for analyzing geospatial data and gaining insights in Geographical Information Science (Corcoran et al. 2023). The ability of persistent homology to characterize complex data structures across multiple scales, as surveyed by Wei et al. 2025, suggests its applicability to analyzing large-scale infrastructure networks derived from sources like OSM.

Specifically, persistent homology can be used to quantify the connectivity patterns, identify cycles (loops), and potentially detect structural vulnerabilities within the road network, the waterway network, or their interaction. For flood risk analysis, TDA offers a framework to analyze how the proximity and spatial arrangement of roads relative to waterways influence the overall network topology, potentially revealing areas prone to disconnection or isolation during flood events based on structural characteristics rather than purely simulation-based or historical methods. This aligns with the objective of the current study to leverage persistent homology and OSM data for flood-prone road prediction based on proximity scoring.

2.4 Flood Risk Assessment Methodologies

Assessing flood risk is paramount for effective urban planning, disaster mitigation, and emergency response, particularly given the increasing impacts of climate change and urbanization (Kundzewicz et al. 2013). A variety of methodologies have been developed to identify flood-prone areas, estimate potential damages, and inform management strategies. These approaches range from detailed physics-based simulations to data-driven statistical models and qualitative assessments.

- **Hydrological and Hydraulic (Hydrodynamic) Models** represent a cornerstone of detailed flood analysis. These models simulate the physical processes of water movement, including rainfall-runoff, channel flow, and inundation over floodplains (Teng et al. 2012). They rely on fundamental physical equations and require detailed input data, including high-resolution Digital Elevation Models (DEMs), rainfall patterns, river cross-sections or bathymetry, land cover information, and boundary conditions (e.g., flow hydrographs, tidal levels). While capable of providing detailed predictions of flood extent, depth, velocity, and duration, these models are often computationally intensive and demand significant expertise for setup, calibration, and validation (Horritt et al. 2002).
- **Statistical and Machine Learning (ML) Methods** offer alternative, data-driven approaches, particularly for flood susceptibility mapping – identifying areas prone to flooding based on correlations with causative factors. These methods learn patterns from historical flood data (inventories) and various geo-environmental factors. Commonly used input factors include elevation, slope, aspect, distance to rivers/waterways, topographic wetness index (TWI), land use/land cover (LULC), soil type, geology, and rainfall characteristics (Tehrany et al. 2014 and Rahmati et al. 2015). A wide array of ML algorithms have been applied, including logistic regression, frequency ratio, weights of evidence, support vector machines (SVM), decision trees (like Random Forests), artificial neural networks (ANN), and increasingly, deep learning techniques like Convolutional Neural Networks (CNNs) (Mosavi et al. 2018 and Zhao et al. 2018). These methods can capture complex, non-linear relationships and may be applicable even when detailed hydraulic data is scarce. However,

their performance heavily depends on the quality and quantity of training data (especially historical flood locations), and they might lack the direct physical interpretability of process-based models.

- **Index-Based Methods and Multi-Criteria Decision Analysis (MCDA)** provide frameworks for combining multiple factors influencing flood risk, often incorporating expert judgment alongside quantitative data. Techniques like the Analytical Hierarchy Process (AHP) are used to assign weights to different factors (e.g., proximity to river, elevation, population density, infrastructure value) based on their perceived importance (Fernandez et al. 2010). These factors are then combined, often within a GIS environment, to create composite risk indices or maps. While relatively straightforward to implement and flexible in incorporating diverse criteria, these methods can be subjective due to their reliance on expert weighting and may simplify the underlying physical processes.

- **Remote Sensing** plays a crucial role across flood risk assessment methodologies. Satellite and airborne sensors provide essential input data, such as DEMs (from LiDAR, InSAR, or photogrammetry) and LULC maps (from optical sensors like Landsat, Sentinel-2). Furthermore, remote sensing is invaluable for mapping actual flood extents during or after events, using optical imagery (where cloud cover permits) or Synthetic Aperture Radar (SAR) systems (like Sentinel-1, TerraSAR-X, RADARSAT), which can penetrate clouds and operate day or night (Mason et al. 2012 and Schumann et al. 2016). This flood extent data is critical for calibrating/validating hydraulic models, training ML models, and assessing impacts.

2.5 Topological Data Analysis in Geospatial and Network Science

Beyond persistent homology, the broader field of Topological Data Analysis (TDA) offers a range of tools designed to uncover the underlying shape, structure, and connectivity within complex datasets. These methods are increasingly finding applications in analyzing geospatial data and networks, providing insights complementary to traditional statistical or graph-theoretic approaches.

TDA techniques, including persistent homology and related methods, are particularly well-suited for **network analysis**. Traditional graph theory focuses on pairwise connections (edges) and metrics based on paths or local neighborhoods. TDA allows for the study of higher-order structures and global connectivity patterns within networks. For instance, by building simplicial complexes (like clique complexes) on top of graphs, TDA can analyze multi-node interactions and identify higher-dimensional holes or cycles (H_k for $k > 1$) that standard graph metrics might miss.

In **geospatial data analysis**, TDA offers novel ways to quantify shape and structure. Persistent homology, as discussed previously, can analyze point clouds (e.g., from LiDAR) or functions defined over spatial domains (e.g., elevation data to identify pits, peaks, passes). Beyond point clouds and DEMs, TDA can be applied to:

- Characterize the shape and complexity of geographic features like coastlines or administrative boundaries (potentially relevant for gerrymandering detection).
- Analyze spatial point patterns to identify clustering, regularity, or the presence of significant voids.
- Study movement data by analyzing the topology of trajectories or flows.
- Analyze remote sensing imagery by characterizing the shape and connectivity of land cover patches or textural patterns.

The work by Corcoran et al. (2023) specifically highlights the potential and applicability of persistent homology within Geographical Information Science (GIS), demonstrating its utility for analyzing spatial point patterns and tracking features in spatio-temporal data.

In summary, TDA provides a powerful mathematical framework for exploring the structure of complex systems like geospatial datasets and networks. Acknowledging that comprehensive flood prediction typically relies on multi-parameter models, often utilizing machine learning techniques, this work presents a focused, prototype investigation using persistent homology. We deliberately selected a single key parameter, distance to the nearest waterway, not to build a predictive model in the traditional sense, but specifically to define the filtration process central to the persistent homology analysis of Bangkok's road network. The contribution of this approach lies not merely in assigning a potential risk level to individual roads based solely on proximity, but in revealing the emergent, multi-scale connectivity structure. Persistent homology allows us to identify how roads group into connected components at various proximity levels. This exposes potentially vulnerable networks of roads that might be simultaneously affected due to their connectivity and proximity to water, as well as potentially resilient or strategically useful connected routes (e.g., those maintaining connectivity far from waterways), offering insights relevant for transportation planning and overall network assessment that complements traditional area-based risk identification.

Chapter 3
Research Methodology

This chapter details the step-by-step process undertaken to achieve the research objectives outlined previously. The methodology integrates geospatial data acquisition and processing, feature engineering based on proximity analysis, and topological data analysis using persistent homology. The overall workflow for data preparation is summarized in Figure 3.1, while the workflow for analyzing the data using persistent homology and applying the findings to flood management is illustrated in Figure 3.2.

3.1 Data Acquisition and Preprocessing

Geospatial data representing the road and waterway infrastructure networks forms the foundation of this analysis.

3.1.1 Road Network Extraction

The road network data for Bangkok was acquired programmatically from OpenStreetMap using OSMnx, a Python library designed for downloading, constructing, analyzing, and visualizing street networks from OSM data. OSMnx simplifies the process of obtaining network data, representing it as NetworkX graph objects, which facilitates further analysis.

Initially, comprehensive road network data encompassing various OpenStreetMap (OSM) highway classifications was acquired for the study area. To align with the study's focus on significant transportation routes potentially impacted by flooding, specific filtering criteria were applied to refine the dataset, ensuring the analysis included road segments classified as `highway=trunk, primary, secondary, tertiary`, or `highway=unclassified`, which represent the primary and secondary road infrastructure. Several categories were explicitly excluded to focus the analysis and manage computational load. Specifically, `highway=residential` roads were omitted to concentrate on principal arterial and connector routes—reflecting the assumption that disruptions to these major corridors are of primary concern for applications like emergency logistics and evacuation planning—while also reducing network complexity. Furthermore, `highway=motorway` segments were excluded based on the assumption that their typical design standards, often including higher elevations and advanced drainage, render them less susceptible to the surface flooding scenarios considered in this study compared to other road classes. Other minor classifications, such as `highway=service, footway, cycleway`, and `highway=path`, were also excluded as they fall outside the scope of major vehicular routes pertinent to this analysis.

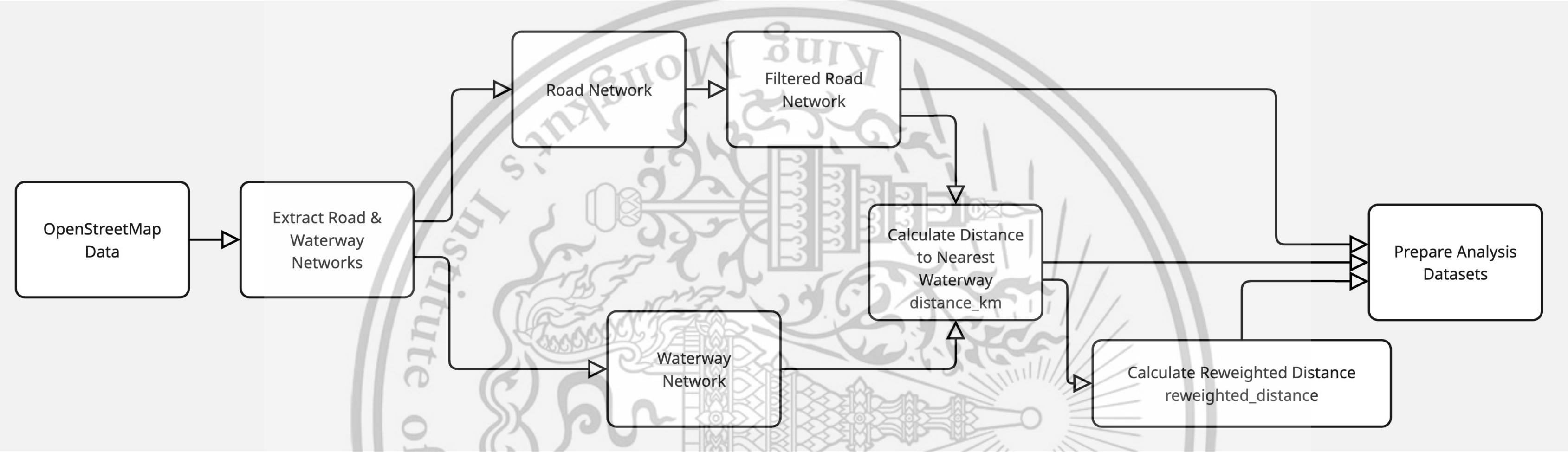

Figure 3.1 Workflow diagram illustrating the data preparation process, from OpenStreetMap data acquisition for Bangkok networks to the generation of analysis-ready datasets including calculated distance parameters

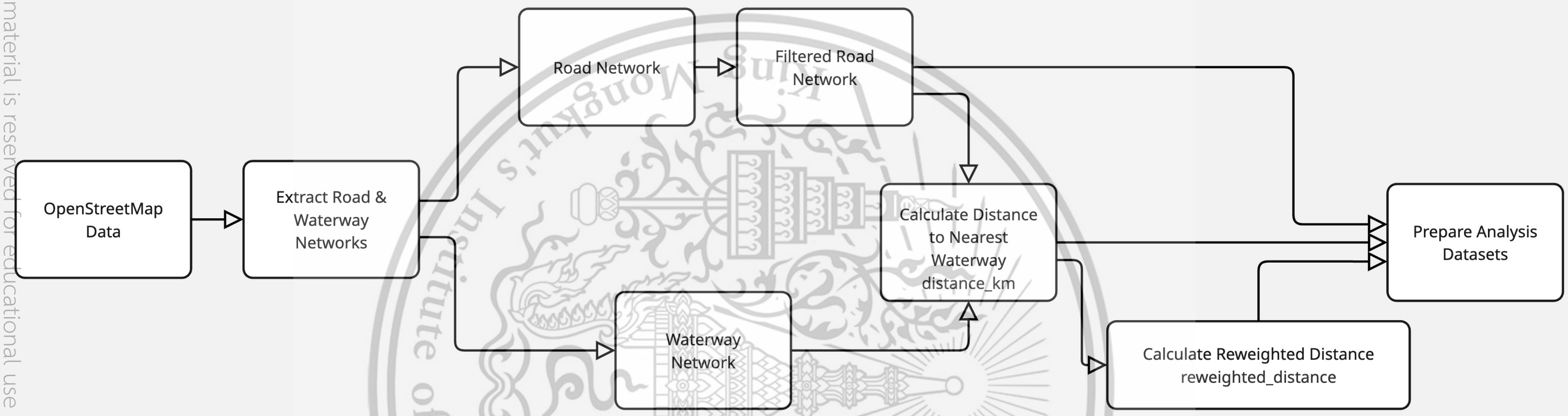

Figure 3.2 Workflow diagram outlining the persistent homology analysis pipeline using both filtration parameters, including result visualization, interpretation, and the subsequent application of findings to flood management contexts in Bangkok.

We obtain the data with the $12,967$ rows and 16 columns:

- u: The starting node ID (OpenStreetMap ID) of the road segment.
- v: The ending node ID (OpenStreetMap ID) of the road segment.
- key: Identifier distinguishing parallel edges, usually 0 if only one edge exists.
- osmid: The OpenStreetMap ID of the original way (road) this segment belongs to.
- name: The official or common name of the road (e.g., ถนนสุขุมวิท).
- highway: The classification type of the road (e.g., primary, tertiary, residential).
- oneway: Indicates if the road segment allows traffic in only one direction (True/False).
- length: The length of the road segment in meters.
- lanes: The number of traffic lanes on the road segment. ref: Any reference number or code assigned to the road (e.g., AH2, 34).
- geometry: The actual shape and location of the road segment (usually a LineString).
- maxspeed: The posted maximum speed limit (often needs unit interpretation, e.g., 60).
- bridge: Indicates if the segment is part of a bridge (e.g., yes).
- access: Specifies any access restrictions (e.g., private).
- tunnel: Indicates if the segment is part of a tunnel (e.g., yes).
- junction: Describes if the segment is part of a junction like a roundabout.
- width: The approximate width of the road segment.

The `geometry` column for each road edge contains a LineString defining its shape using latitude-longitude coordinates e.g. `LINESTRING (100.6433283 13.6612042, 100.6432324 13.6614331, 100.6430951 13.6616082, 100.6427775 13.6619919)`. These LineStrings often include multiple intermediate nodes along the road segment. We focused on the endpoints of each edge, storing their identifiers in the `beginning_node` and `ending_node` columns.

3.1.2 Waterway Network Extraction

Waterway data for Bangkok was also sourced from OpenStreetMap. Similar to the road network, specific types of waterways deemed most relevant to potential surface flooding and interaction with the road network were selected. These include features tagged in OSM as: `waterway=river,drain,ditch,canal`. Other waterway types (e.g., small streams, culverts represented as points) were excluded from this analysis.

We obtain the data with the $2,208$ rows and 10 columns:

- u: The starting node ID (OpenStreetMap ID) of the waterway segment.
- v: The ending node ID (OpenStreetMap ID) of the waterway segment.
- key: Identifier distinguishing parallel edges, usually 0 if only one edge exists.
- osmid: The OpenStreetMap ID of the original way (waterway) this segment represents.
- name: The official or common name of the waterway (e.g., คลองแสนแสบ). May be absent.
- oneway: Indicates if flow is restricted to one direction (True/False). Often False/absent for natural rivers, can be True for canals.
- length: The length of the waterway segment in meters.
- geometry: The actual shape and location of the waterway segment (usually a LineString).
- width: The approximate or specified width of the waterway segment in meters.
- tunnel: Indicates if the waterway segment passes through a tunnel or culvert (e.g., yes, culvert).

3.1.3 Visualization

We use the NetworkX Python library to visualize both the road and waterway networks.

- **Nodes** represent junctions or intersections.
- **Edges** represent the road segments or waterway segments connecting these junctions.

We create nodes based on unique coordinates (`starting_point` and `ending_point`). There are $7,009$ unique coordinates in the CSV file. We create edges based

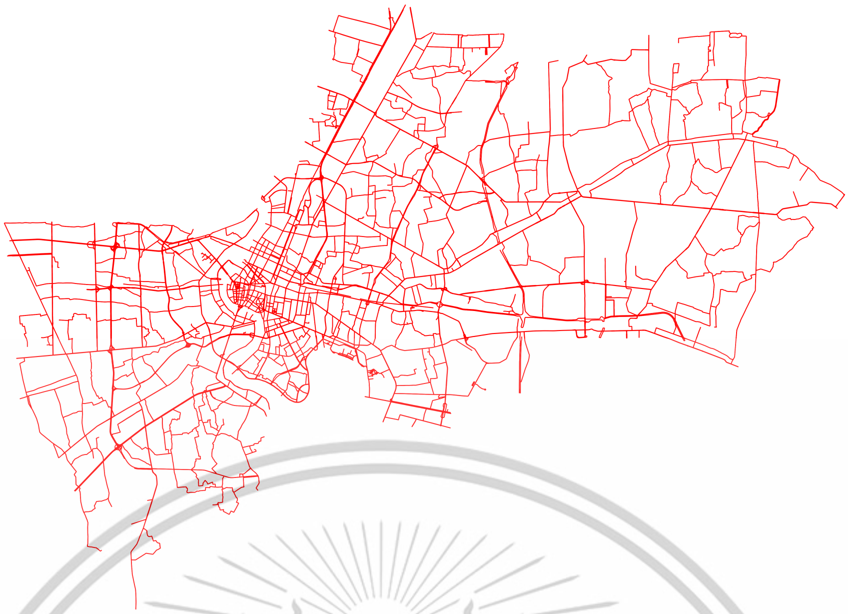

Figure 3.3 Visualization of the Bangkok road network derived from OSM data.

on unique $9,099$ edges. This means that multiple rows in the CSV file (from $12,966$ rows) refer to the same edge in the graph (same starting and ending coordinates). See Figure 3.3, Figure 3.4 and Figure 3.5.

3.2 Feature Engineering: Proximity to Waterways

A key aspect of this methodology is quantifying the flood risk potential based on proximity. To achieve this, a custom function was developed in Python to calculate the minimum Euclidean distance from each road edge in the selected LCC to the nearest waterway edge (from the filtered waterway dataset).

For each road edge (represented by its line geometry), the algorithm iterates through all waterway edges, calculates the shortest distance between the road edge geometry and the waterway edge geometry, and identifies the minimum distance found. This minimum distance value, representing the closest proximity of that specific road segment to a relevant waterway, was then appended as a new attribute to the road edge data.

Defined two distinct weighting schemes for each road segment (edge) based on its proximity to the nearest waterway:

1. Higher weight for greater distance: Assigned progressively larger weights to roads located further from the nearest waterway. The minimum distance between a road edge and a waterway edge is computed using *Shapely's distance method*, which calculates the shortest distance between two geometric objects. Let $P_1 = (\text{lon}_1, \text{lat}_1)$ and $P_2 = (\text{lon}_2, \text{lat}_2)$ be two points where lat_i

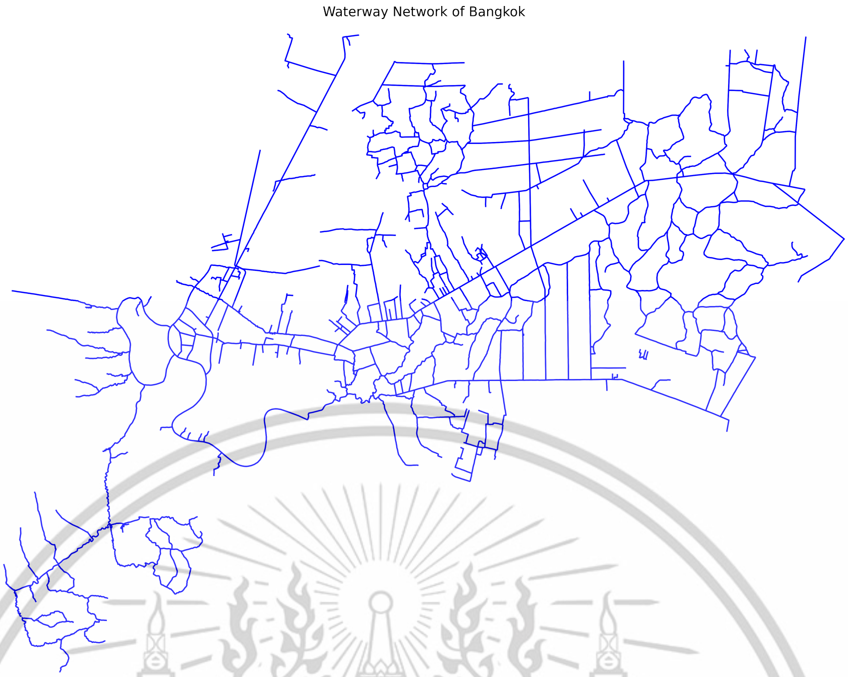

Figure 3.4 Visualization of the Bangkok waterway network derived from OSM data.

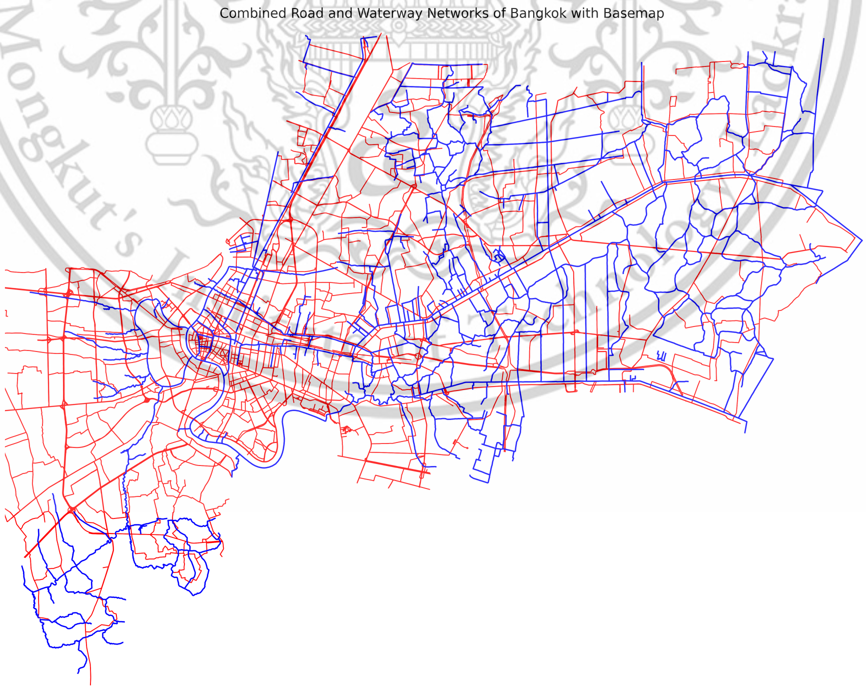

Figure 3.5 Visualization of the combined road and waterway networks of Bangkok, derived from OSM data.

is latitude of P_i and lon_i is longitude of P_i for $i = 1, 2$. The formula that we use to calculate the distance (in degree) between the two closest points is $P_1 = (\text{lon}_1, \text{lat}_1)$ and $P_2 = (\text{lon}_2, \text{lat}_2)$ on the two geometries is

$$\text{distance\_degree} = \sqrt{(\text{lon}_2 - \text{lon}_1)^2 + (\text{lat}_2 - \text{lat}_1)^2}.$$

Then convert to kilometers using the approximation:

$$\text{distance\_km} = \text{distance} \times 111.32.$$

We calculate and add these information to the columns named `distance_degrees` and `distance_km`.

2. Lower weight for greater distance: Assigned progressively smaller weights to roads located further from the nearest waterway. For each edge in the road network, we define its weight using the decreasing function

$$\text{reweighted\_distance} = 19 - \text{distance\_km}.$$

To ensure that reweighted_distance remains positive, this function was chosen due to the maximum observed `distance_km` is 18.719. We calculate and add this information to the column named `reweighted_distance`.

3.2.1 Processed Dataset

The processed dataset consists of road network edges, each associated with its geometric information, original OSM attributes, and the newly computed distance to waterway attribute. The key columns include:

1. Road edge information
    - road_edge_index
    - road_edge_id
    - beginning_node
    - ending_node
    - road_name
2. Corresponding nearest waterway edge information
    - waterway_edge_index
    - waterway_edge_id
    - waterway_name
3. Distance
    - distance_degrees
    - distance_km
    - reweighted_distance

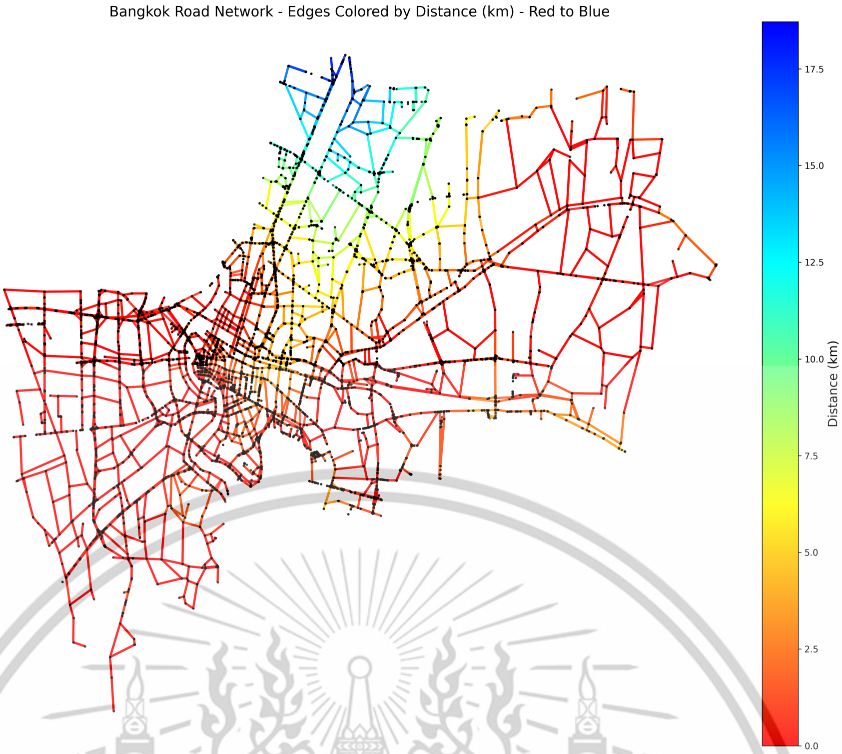

Figure 3.6 Visualization of the Bangkok road network highlighting proximity to waterways. Road segments are colored on a spectrum from red (closest to waterway) to blue (farthest from waterway)

3.2.2 Network Merging and Largest Connected Component Selection

The extracted road and waterway datasets, consisting of nodes (geographic points) and edges (lines connecting nodes with associated geometry), were processed. To ensure the analysis focused on the main, interconnected part of the transportation network, *the Largest Connected Component (LCC)* of the filtered road network graph was identified and selected for subsequent analysis. This step removes isolated road segments or small, disconnected network clusters which are less critical for understanding city-wide connectivity patterns relevant to large-scale flooding impacts. Largest component has

- 6,542 nodes (93.34% of the original nodes)
- 8,749 edges (96.15% of the original edges)

The LCC typically contains the vast majority of the network's nodes and edges. Focusing on the LCC is justified as disruptions within this major component have the most significant implications for mobility and logistics during flood events.

3.3 Persistent Homology Analysis

3.3.1 Filtration

We use clique complex filtration to analyze the persistence homology. Creates a sequence of nested simplicial complex from an initial weighted graph.

1. Higher weight for greater distance (`distance_km`)

2. Lower weight for greater distance (`reweighted_distance`)

Typically built by adding edges progressively based on edge weights in order of increasing weight. If edges form a complete graph, its interior is immediately filled.

3.3.2 Computation using GUDHI

The computation of persistent homology for the constructed filtration was performed using the GUDHI library, accessed via its Python bindings. GUDHI (Geometry Understanding in Higher Dimensions) is an open-source library offering robust and efficient algorithms for computational topology and geometric inference.

Persistent homology was computed for dimension $k = 0$. H_0 (Zeroth Homology) tracks the appearance and merging of connected components in the network as the distance threshold ϵ increases. Birth times (b) correspond to the distance value at which a road segment (or component) appears, and death times (d) correspond to the distance value at which two previously separate components merge. Calculations were performed using coefficients in $\mathbb{Z}_2$ for simplicity.

3.4 Output Visualization and Interpretation

The output of the persistent homology computation consists of persistence pairs (b, d) for each identified topological feature, representing the feature's birth (b) and death (d) values according to the chosen filtration parameter which are `distance_km` and `reweight_distance`). To analyze these results, standard topological data analysis (TDA) visualization tools were employed:

1. **Persistence Barcodes**: These visualizations depict each topological feature (specifically H_0 features, representing connected components in this context) as a horizontal bar $[b, d)$. The length of the bar ($d - b$) visually represents the feature's persistence across the filtration. *Long bars* correspond to features that persist over a wide range of the filtration parameter. For H_0 using `distance_km`, these may indicate core connected components of the road network whose connectivity is stable across significant variations in distance to waterways. *Short bars* represent features with short lifetimes (small $d - b$), potentially corresponding to noise, transient structural artifacts, or localized

connectivity patterns highly sensitive to small changes in the filtration parameter threshold.

2. **Persistence Diagrams**: These diagrams provide an alternative visualization, plotting each feature as a point (b, d) in a 2D scatter plot. The diagonal line $y = x$ represents zero persistence. *Points far from the diagonal* represent features with high persistence (large $d - b$), conveying similar information to long bars regarding stable topological structures. *Points close to the diagonal* represent low-persistence features, often interpreted as noise or minor structural details. Analyzing the specific coordinates (b and d) of points far from the diagonal provides quantitative insights into the parameter values at which significant components form and merge. High-persistence H_0 features are particularly indicative of stable connected components relative to the filtration criterion.

3. **Betti Number (β_0) Plot**: A plot was generated showing the zeroth Betti number, β_0 (which counts the number of connected components), as a function of the filtration parameter. The y-axis represents β_0, and the x-axis represents the increasing filtration parameter value. This plot clearly illustrates how connected components merge as the parameter threshold increases, providing a global overview of the connectivity evolution.

4. **Graph Visualizations at Specific Thresholds**: To gain qualitative insights into the network structure at key moments identified by persistent homology, visualizations of the graph itself were generated at specific threshold values. These thresholds were selected using three different strategies to capture distinct aspects of the filtration:

   (a) Evenly Spaced Thresholds: Thresholds selected by dividing the full range of the filtration parameter values (from minimum to maximum observed edge weight) into a predetermined number of equal intervals. This provides snapshots across the entire process.

   (b) Persistence-Based Thresholds: Thresholds corresponding to significant birth or death times of features identified as highly persistent in the persistence diagram. This highlights the graph structure just before or after major topological events.

   (c) Component-Based Thresholds: Thresholds chosen specifically at filtration values where significant changes occur in the number of connected components (β_0), such as major merging events indicated by large drops in the β_0 plot.

Chapter 4
Result and Discussion

This chapter presents the results obtained from applying persistent homology analysis, specifically focusing on the zeroth homology group (H_0), to the filtered Bangkok road network. The analysis was conducted using two distinct filtration parameters derived from the proximity of road segments to waterways: `distance_km` (direct distance) and `reweighted_distance` (inversely related to distance). The visualizations generated through standard Topological Data Analysis (TDA) tools are presented, including persistence barcodes, persistence diagrams, Betti number plots, and graph snapshots at specific thresholds. Subsequently, the chapter discusses the interpretation of these topological features and their potential applications in flood management, risk assessment, and planning within the context of Bangkok.

4.1 Persistent Homology Results: `distance_km` Filtration

The first analysis utilized the direct distance to the nearest waterway (`distance_-km`) as the filtration parameter. In this setup, edges (road segments) are conceptually added to the graph filtration as the distance threshold increases, allowing us to track how components connect based on their proximity to waterways. The key results are visualized below:

4.1.1 Persistence Barcode, Persistent Diagram and Betti Number Plot

Examination of the H_0 persistent homology results for the `distance_km` filtration reveals key characteristics of the road network's connectivity relative to waterways. The persistence barcode (Figure 4.1) prominently displays a high density of short bars originating and terminating at low `distance_km` values. This indicates that numerous connected components form and then quickly merge with others (i.e., exhibit short persistence intervals) when considering roads primarily situated close to waterways.

This observation is consistent with the persistence diagram (Figure 4.2). This confirms that many components are born and subsequently die (merge) at relatively small distances from waterways. Both the barcode and diagram suggest the presence of certain thresholds where numerous bars terminate or points cluster horizontally, indicating significant merging events where many components merge simultaneously around those specific distance values. Furthermore, the persistence diagram indicates that beyond a `distance_km` threshold of approximately 5.0 km, component death events become less frequent, with this trend becoming even more pronounced after approximately 12.0 km, suggesting greater stability of the remaining larger components at increasing distances from waterways.

These structural changes are quantitatively summarized by the β_0 plot (Figure 4.3), which illustrates the number of connected components (β_0) as a function of the distance_km threshold. The plot clearly shows a rapid decrease in β_0 within the initial $0 - 2.5$ km range, reflecting the frequent merging of components close to waterways. Subsequently, distinct, significant drops in the Betti number are observed around the 5.0 km and 11.0 km thresholds. Identifying the precise filtration values corresponding to these major topological changes, potentially using the strategies discussed in the next section, can pinpoint critical distances that significantly alter network connectivity.

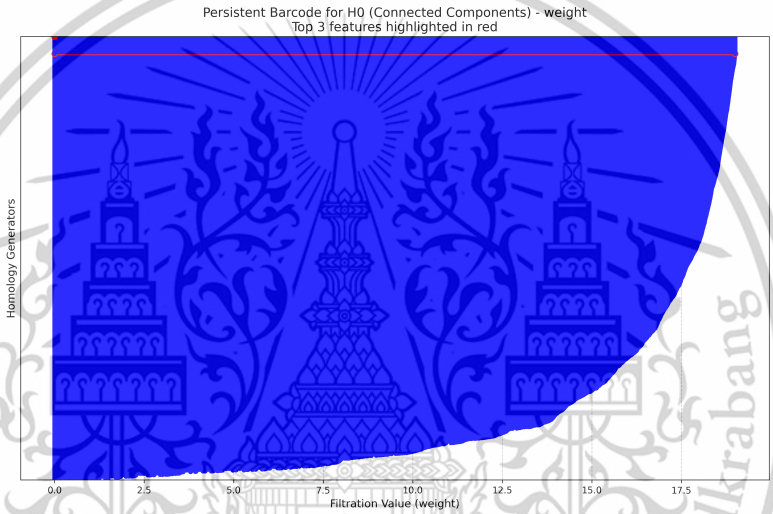

Figure 4.1 Persistence Barcode (H_0) for distance_km Filtration. This barcode displays each connected component (H_0 feature) as a horizontal bar $[b, d)$, where b and d are the distance_km values at which the component appears and merges with an older component. Bar length indicates persistence.

4.1.2 Road Networks at Selected distance_km Thresholds

To provide a qualitative understanding of how the road network's structure evolves during the distance_km filtration, visualizations of the corresponding simplicial complex were generated at specific threshold values. These key thresholds were selected using three distinct strategies.

1. Evenly Spaced Strategy (Figure **??** and **??**: For this approach, the full range of the distance_km filtration parameter was divided into six equal intervals. Four intermediate threshold values representing these intervals were then selected for visualization. This method provides snapshots of the network structure at regular intervals across the filtration, potentially illustrating pro-

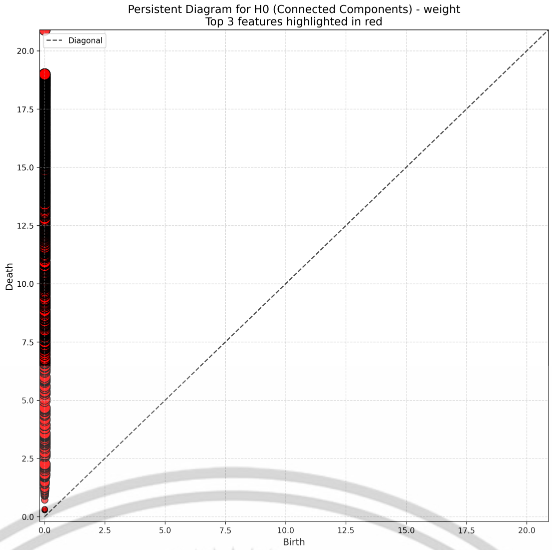

Figure 4.2 Persistence Diagram (H_0) for `distance_km` Filtration. This diagram plots each component feature as a point (b, d). Points far from the diagonal $(y = x)$ represent highly persistent components, stable across a wide range of distances to waterways.

gressive stages related to increasing proximity buffers around waterways.

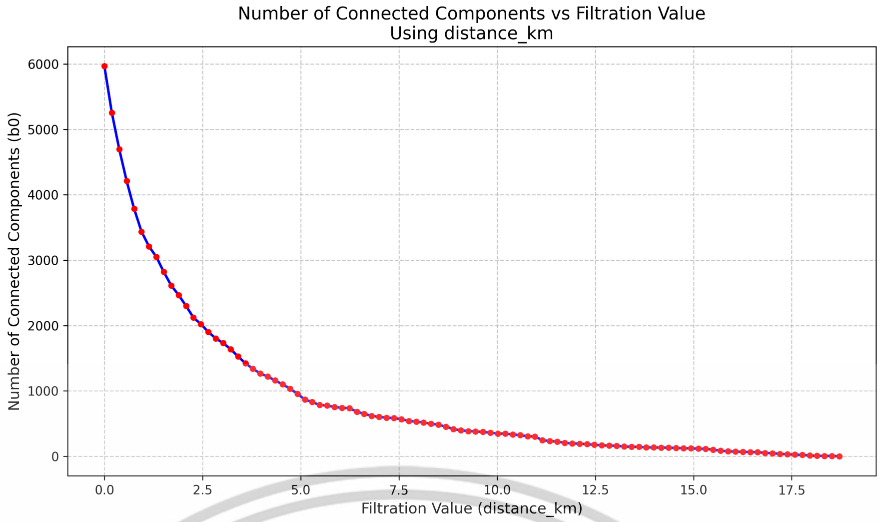

Figure 4.3 Betti Number (β_0) Plot for `distance_km` Filtration. This plot shows the number of connected components (β_0, y-axis) as a function of the `distance_km` filtration parameter (x-axis). Drops in the plot indicate component merging events.

2. Persistence-Based Strategy (Figure 4.6 and 4.7): This strategy focused on identifying thresholds related to significant topological events observed in the persistence diagram (Figure 4.2). Based on the birth or death times of highly persistent H_0 features, the analysis identified key structural transitions occurring near `distance_km` thresholds of approximately $0.3353, 0.8504, 1.9855,$ and 4.2612 km. Visualizing the network at these points highlights the structure around moments of significant topological feature change.

3. Component-Based Strategy (Figure 4.8 and 4.9): Here, thresholds were selected corresponding to filtration values where significant changes (specifically, rapid decreases) occur in the number of connected components (β_0), as indicated by the β_0 plot (Figure 4.8 and 4.9). Key thresholds identified using this method were approximately $0.0004, 0.0279, 0.1017,$ and 0.1520 km. The low values identified by this strategy are consistent with the β_0 plot (Figure 4.3), which indeed shows that the most rapid decrease in the number of connected components occurs at `distance_km` values very close to zero, reflecting the quick merging of components near waterways.

4.2 Persistent Homology Results: `reweighted_distance` Filtration

The second analysis employed the `reweighted_distance` parameter, calculated as $r(d) = 19 - d$ where d is `distance_km`. In this filtration, edges with low `reweighted_distance` correspond to roads far from waterways, and edges with high `reweighted_distance` correspond to roads close to waterways. The standard persistent homology algorithm, applied to increasing `reweighted_distance`, therefore tracks connectivity starting from roads far from water and progressively incorporates those closer.

The H_0 persistent homology results for the `reweighted_distance` filtration reveal a distinct pattern of component evolution. Observing the persistence barcode (Figure 4.10), connected components appear to merge (die) relatively slowly throughout the initial range of the filtration, specifically for `reweighted_distancee` values from 0 up to approximately 15. However, after this point (corresponding to roads closer than approximately 5 km to waterways), the rate of component merging appears to accelerate notably.

This trend is consistent with the persistence diagram (Figure 4.15 and Figure 4.16), which shows a discernible increase in the density of points (b, d) whose death coordinate (d) occurs at `reweighted_distance` values greater than approximately 15. Both the barcode and the diagram suggest a particularly concentrated period of merging activity within the approximate `reweighted_distance` interval of 13.5 to 14.5, where a significant number of components terminate. This dynamic is clearly illustrated by the β_0 plot (Figure 4.12), graphing the number of connected components against the `reweighted_distance` parameter. The curve exhibits a relatively gradual decrease for thresholds below approximately 14, followed by a steeper decline after 15. This confirms the accelerated merging of components as the filtration increasingly incorporates road segments situated closer to waterways (represented by higher `reweighted_distance` values). The precise thresholds related to these significant topological changes are determined using the selection strategies outlined in the next subsequent section.

4.2.1 Road Networks at Selected `reweighted_distance` Thresholds

Visualizations of the simplicial complex corresponding to the `reweighted_-distance` filtration are presented in this section, illustrating the network structure at specific thresholds selected via three distinct strategies.

1. Evenly Spaced Strategy (Figure 4.13 and 4.14): The `reweighted_distance` parameter range was divided into six equal intervals, and four intermediate threshold values were chosen for visualization. This approach allows observation of the network's structural evolution at regular intervals. Given that

lower `reweighted_distance` values correspond to roads farther from waterways, these snapshots may help visualize the formation of potentially more resilient or safer networks at different stages.

2. Persistence-Based Strategy (Figure 4.15 and 4.16): Thresholds were selected near significant topological events (births or deaths of highly persistent H_0 features). Key thresholds highlighted by this strategy occurred around `reweighted_distance` values of $14.7768, 17.0121, 18.1218$, and 18.6350. Visualizing the network at these points reveals the structure around critical moments of topological change in the reweighted space.

3. Component-Based Strategy (Figure 4.17 and Figure 4.18): This strategy identified thresholds corresponding to significant drops in the number of connected components (β_0), derived from the β_0 plot (Figure 4.12). The selected `reweighted_distance` thresholds occurred near $0.2870, 17.4824, 18.7029$, and 18.8988. The identification of several significant merging thresholds at high `reweighted_distance` values (especially > 17) using this method is consistent with the β_0 plot (Figure 4.12), which shows pronounced decreases in the number of components occurring particularly after the threshold of approximately 15.

4.3 Implications for Flood Management

The topological insights gained from the persistent homology analyses offer valuable perspectives for flood management in Bangkok. Evaluating road networks based on parameters related to flood susceptibility, such as the distance metrics used here to drive the filtrations, enables the identification of structural vulnerabilities and potentially resilient segments at different conceptual risk levels. This identification is crucial for improving flood prediction models, facilitating proactive planning efforts, and developing effective intervention strategies.

4.3.1 Flood Risk Identification (using `distance_km`)

The analysis using direct distance to waterways (`distance_km`) effectively tracks the formation and merging of connected road components situated at increasing distances from water sources. Features observed at lower distance thresholds, specifically components merging when considering roads close to waterways, can potentially indicate connected road networks that might be at higher risk of simultaneous flooding due to proximity. This topological perspective offers insights that can augment traditional flood models. For instance, roads identified as part of components existing only at low `distance_km` thresholds could be flagged for further investigation or prioritized in risk assessments. Figure 4.19 provides an example visualization of such network components present at a low `distance_km` threshold. Furthermore, this approach enables the extraction of specific road segment data associated with the components present at any given `distance_km` threshold. By interpreting the `distance_km` parameter as a proxy for flood-proneness (where lower values imply higher potential exposure), one can identify which specific roads constitute these potentially vulnerable networks at various proximity-to-water levels.

Example 4.3.1. This figure illustrates the connected components formed by roads within approximately 0.3353 km of a waterway. Furthermore, Figure 4.20 provides an example visualization showing road segments that belong to components identified as potentially high-risk corresponding to this threshold.

4.3.2 Identification of Potentially Usable Routes (using `reweighted_distance`)

The analysis using `reweighted_distance` tracks connectivity differently, effectively prioritizing connections between roads farther from waterways first in the standard filtration process. Features observed in this filtration, particularly components that form early (low `reweighted_distance`) or persist across ranges corresponding to larger distances from water, could potentially highlight connected road networks that may remain usable longer during flooding events or are generally less susceptible. This information could be valuable for planning evacuation routes or identifying critical infrastructure corridors likely to maintain connectivity. Figure 4.21 shows an example network structure at a specific `reweighted_distance` threshold. The data associated with edges forming such stable components (e.g., `road_edge_index`, `road_edge_id`, `road_name`, `reweighted_distance`) can be extracted for planning purposes.

Example 4.3.2. This figure shows the network components present when considering roads up to a reweighted distance score of 14.7768 (corresponding to roads with a direct distance $d = 19–14.7768 = 4.2232$ km or more from waterways). Furthermore, the specific road segments constituting the network structure at this 14.7768 `reweighted_distance` threshold are detailed in Figure 4.22.

4.3.3 Establishing Flood Trigger Levels

The persistent homology framework can help inform the establishment of critical thresholds for flood response. Significant filtration values where major topological changes occur (e.g., the death times of highly persistent features from the persistence diagram, or thresholds identified via the component-based strategy causing large drops in β_0) represent points where the network's connectivity fundamentally shifts relative to the filtration parameter. These data-driven topological thresholds could potentially serve as candidates for *Flood Trigger Levels*. Applying this concept, if real-world monitoring (such as predicted flood extent) indicates that areas corresponding to roads associated with a critical, PH-derived `distance_km` threshold (one signifying significant connectivity changes) are impacted, this could serve as a data-driven signal to activate specific response plans or escalate interventions—moving from routine monitoring (small plan) towards more comprehensive actions (bigger plan). For example, understanding the network structure just before a major component merging event, as identified via persistence or β_0 analysis, provides valuable insight into such a critical state transition.

Example 4.3.3. Figure 4.21 displays the simplicial complex representing the network structure at the `reweighted_distance` threshold of 14.7768, a value identified as topologically significant using the persistence-based selection strategy. The occurrence of a major topological transition at this specific threshold—which incorporates connectivity information primarily involving roads situated approximately $19-14.7768 = 4.2232$ km or further from waterways—might suggest that conditions leading to such widespread network changes could correspond to a critical or severe flooding scenario.

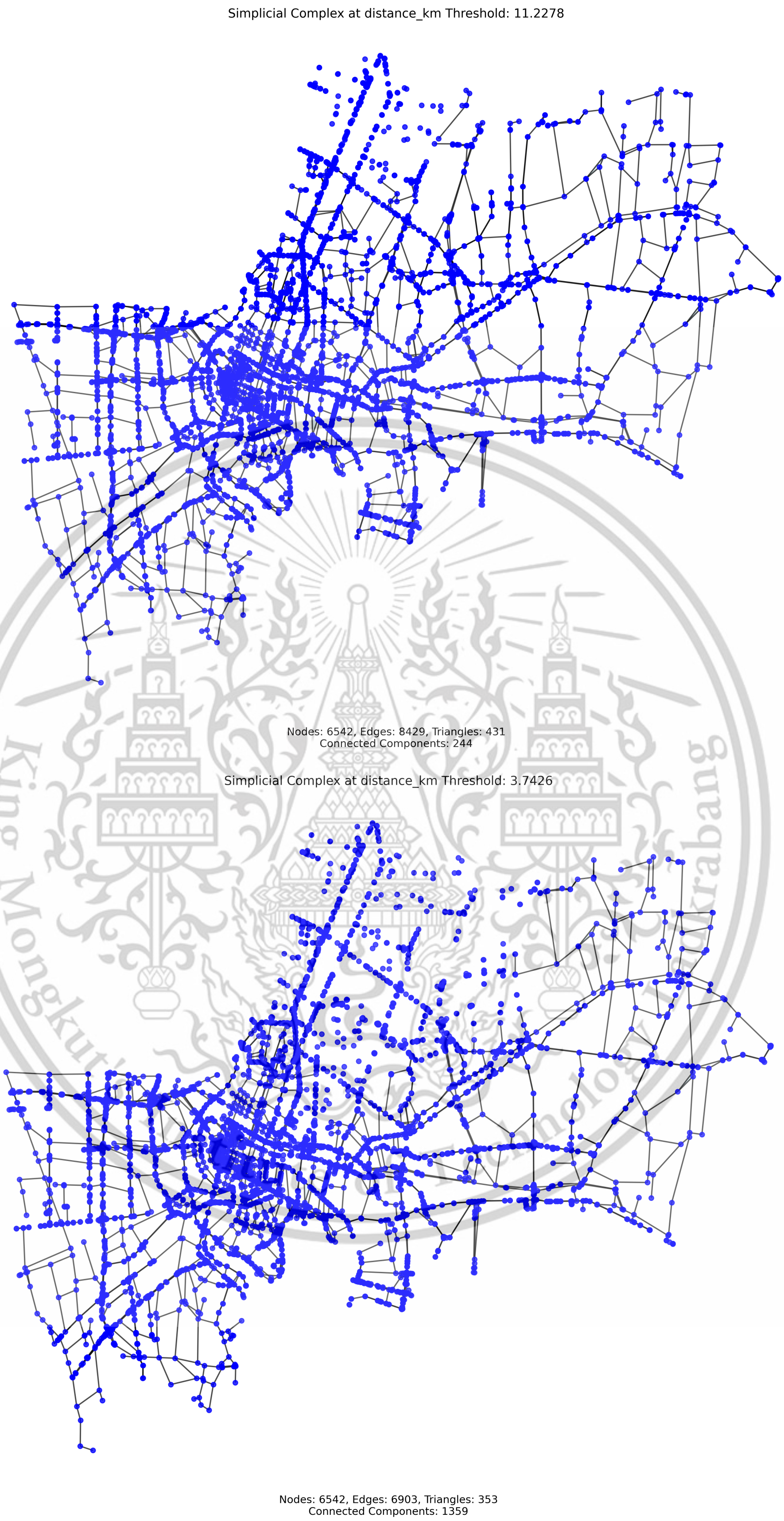

Figure 4.4 Visualization of the simplicial complex representing the Bangkok road network at four thresholds for the `distance_km` parameter which are $\texttt{distance\_km} = 3.7426$ and 7.4852, respectively, selected using the evenly strategy across the parameter range.

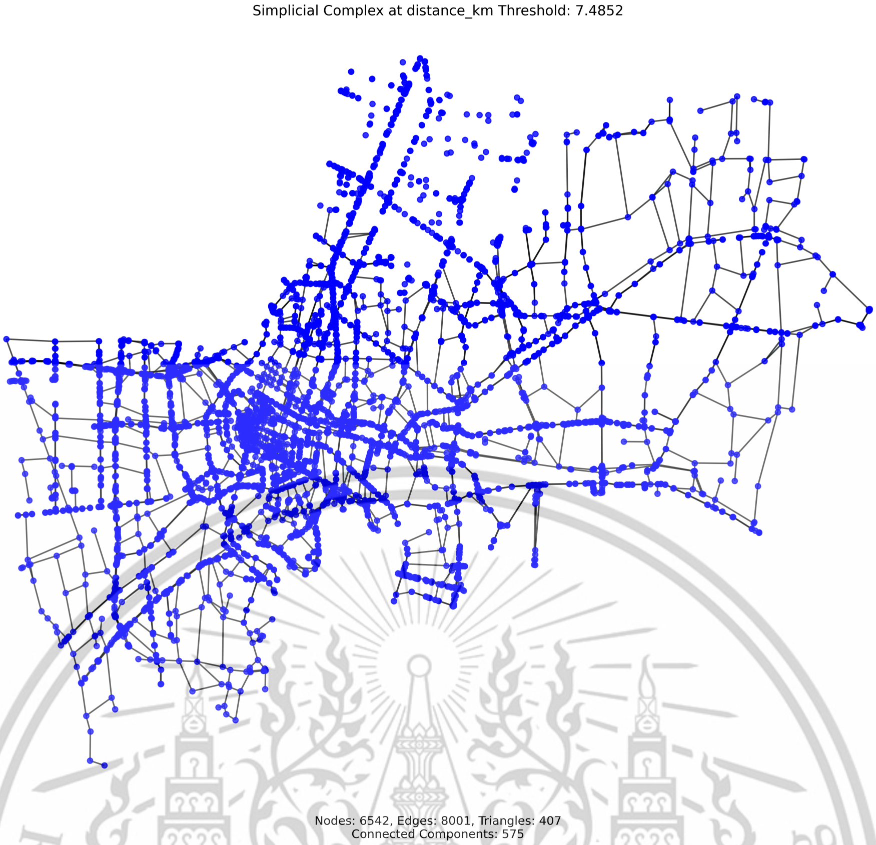

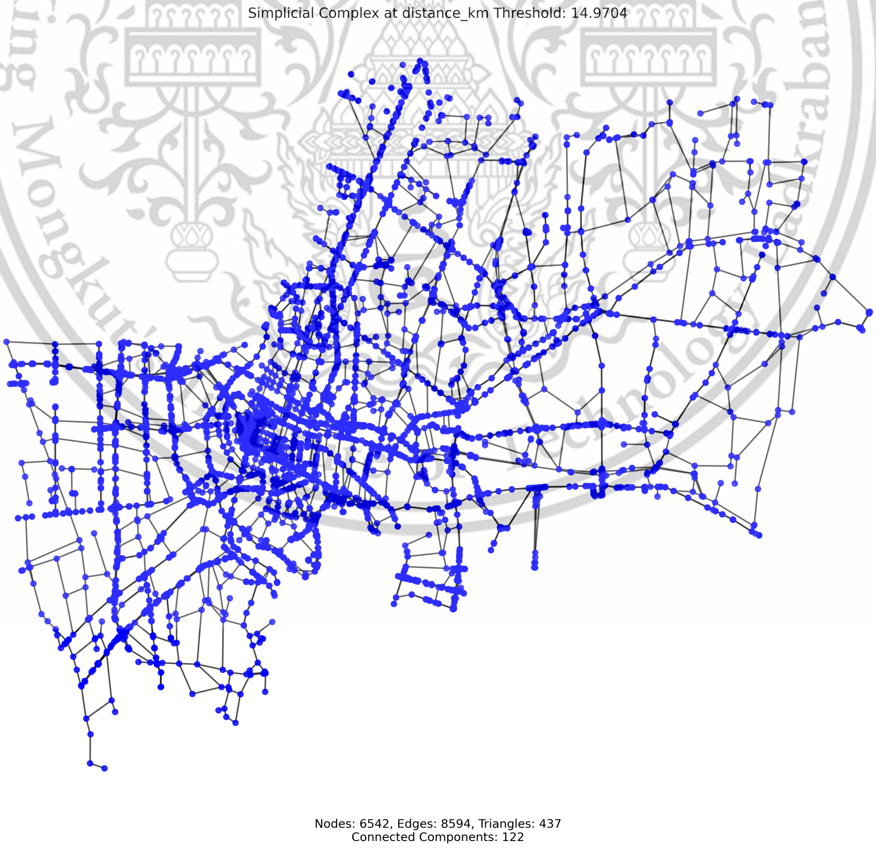

Figure 4.5 Visualization of the simplicial complex representing the Bangkok road network at four thresholds for the **distance_km** parameter which are **distance_km** $= 11.2278$ and 14.9704, respectively, selected using the evenly strategy across the parameter range.

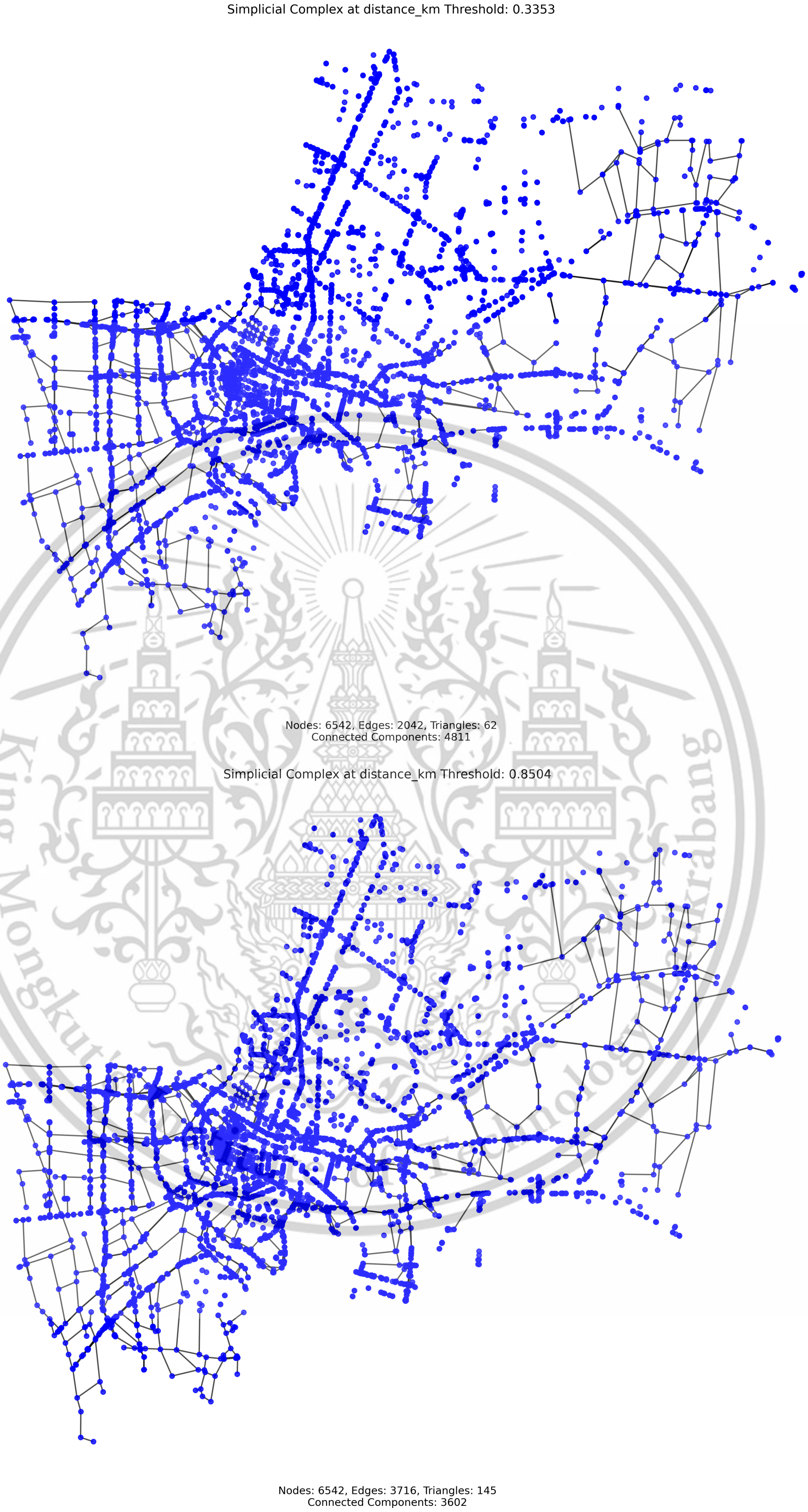

Figure 4.6 Visualization of the simplicial complex representing the Bangkok road network at four thresholds for the `distance_km` parameter which are `distance_km` $= 0.3353$ and 0.8504, respectively, selected using the persistence-based strategy across the parameter range.

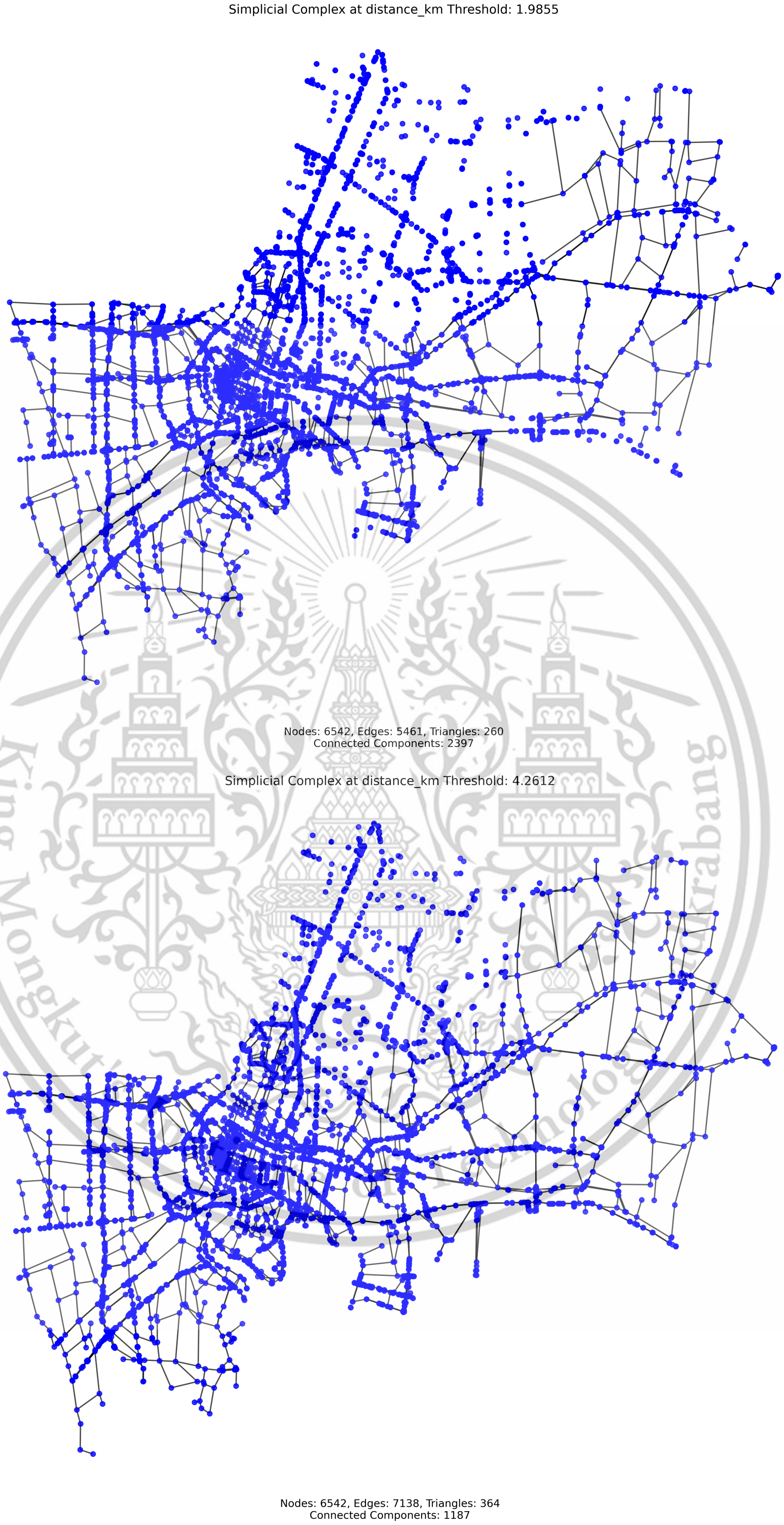

Figure 4.7 Visualization of the simplicial complex representing the Bangkok road network at four thresholds for the `distance_km` parameter which are `distance_km` $= 1.9855$ and 4.2612, respectively, selected using the persistence-based strategy across the parameter range.

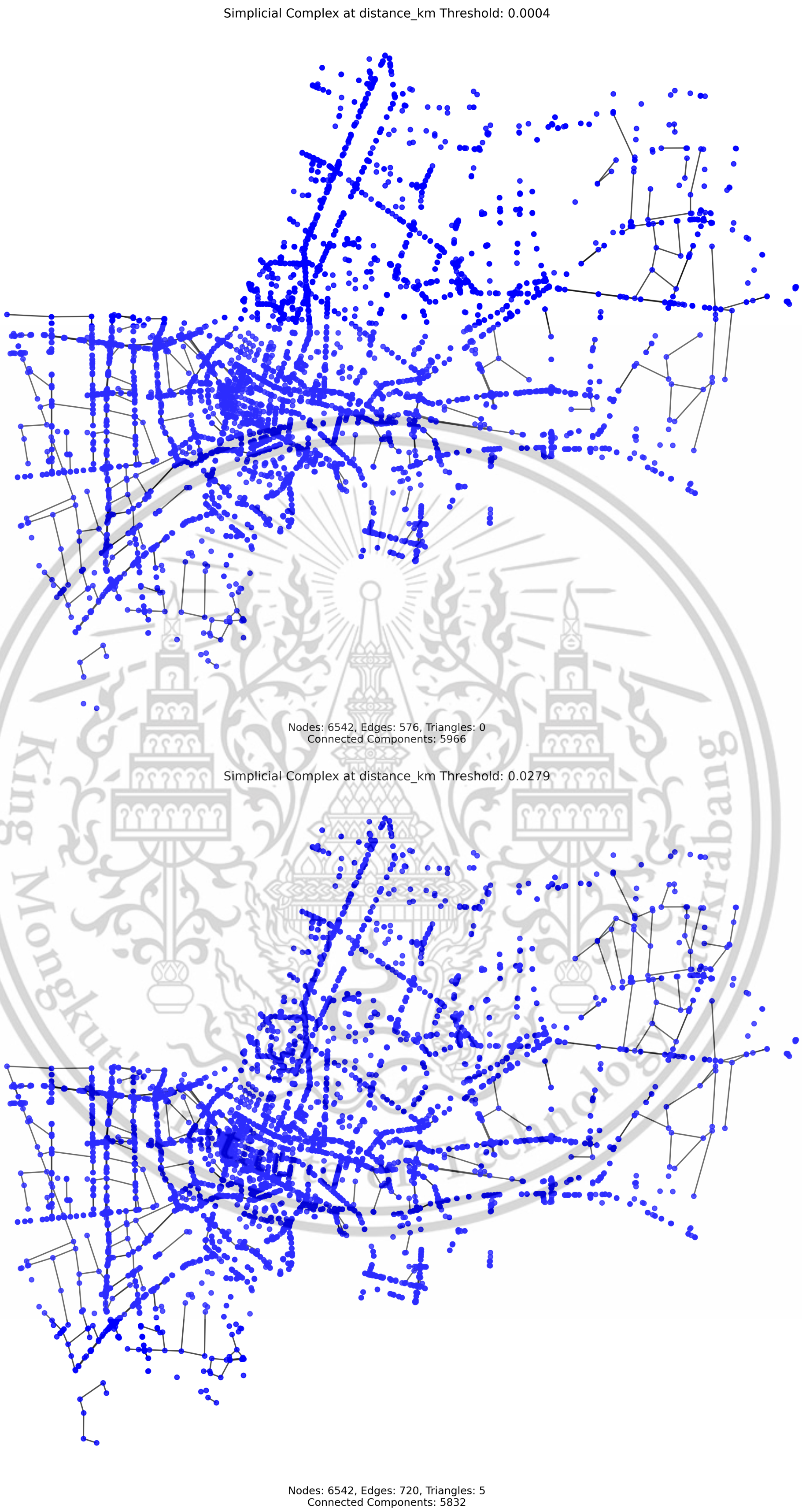

Figure 4.8 Visualization of the simplicial complex representing the Bangkok road network at four thresholds for the `distance_km` parameter which are `distance_km` $= 0.0004$ and 0.0279, respectively, selected using the component-based strategy across the parameter range.

Figure 4.9 Visualization of the simplicial complex representing the Bangkok road network at four thresholds for the `distance_km` parameter which are `distance_km` $= 0.1017$ and 0.1520, respectively, selected using the component-based strategy across the parameter range.

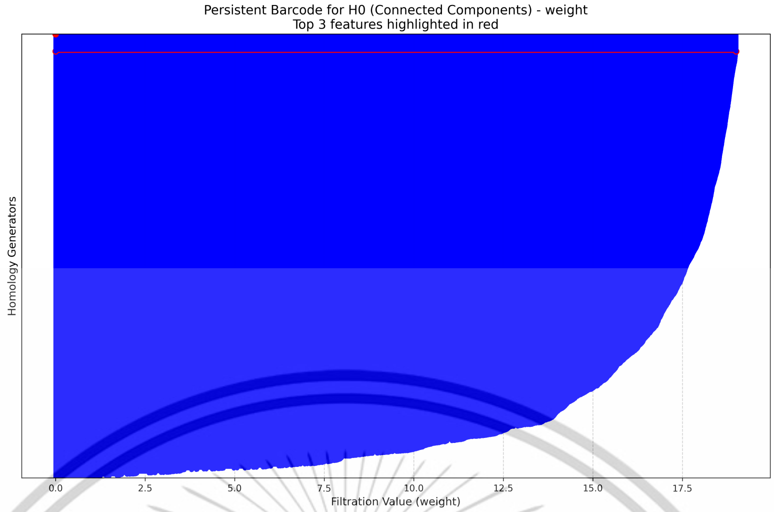

Figure 4.10 Persistence Barcode (H_0) for `reweighted_distance` Filtration. This barcode displays each connected component (H_0 feature) as a horizontal bar $[b, d)$, where b and d are the `reweighted_distance` values at which the component appears and merges with an older component. Bar length indicates persistence.

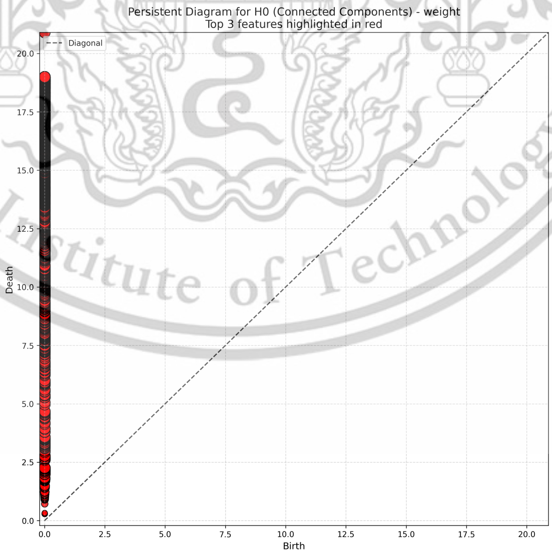

Figure 4.11 Persistence Diagram (H_0) for `reweighted_distance` Filtration. This diagram plots each component feature as a point (b, d). Points far from the diagonal ($y = x$) represent highly persistent components, stable across a wide range of distances to waterways.

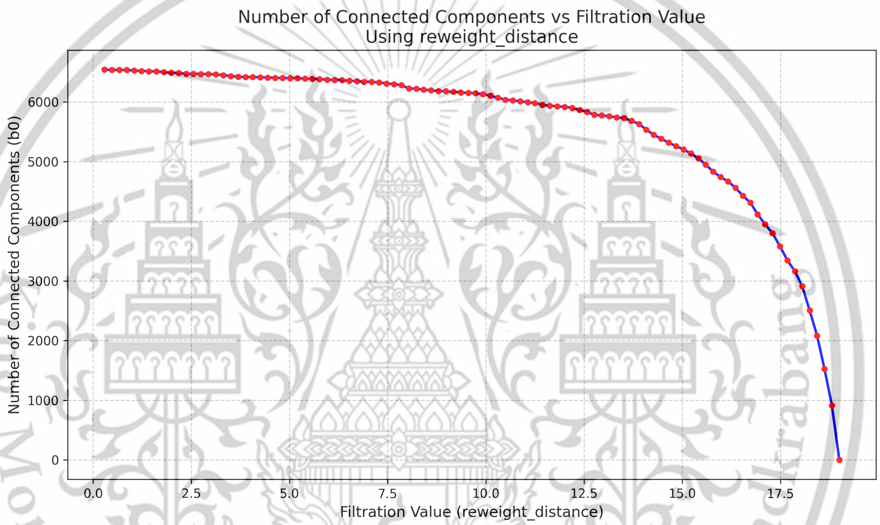

Figure 4.12 Betti Number (β_0) Plot for `reweighted_distance` Filtration. This plot shows the number of connected components (β_0, y-axis) as a function of the `reweighted_-distance` filtration parameter (x-axis). Drops in the plot indicate component merging events.

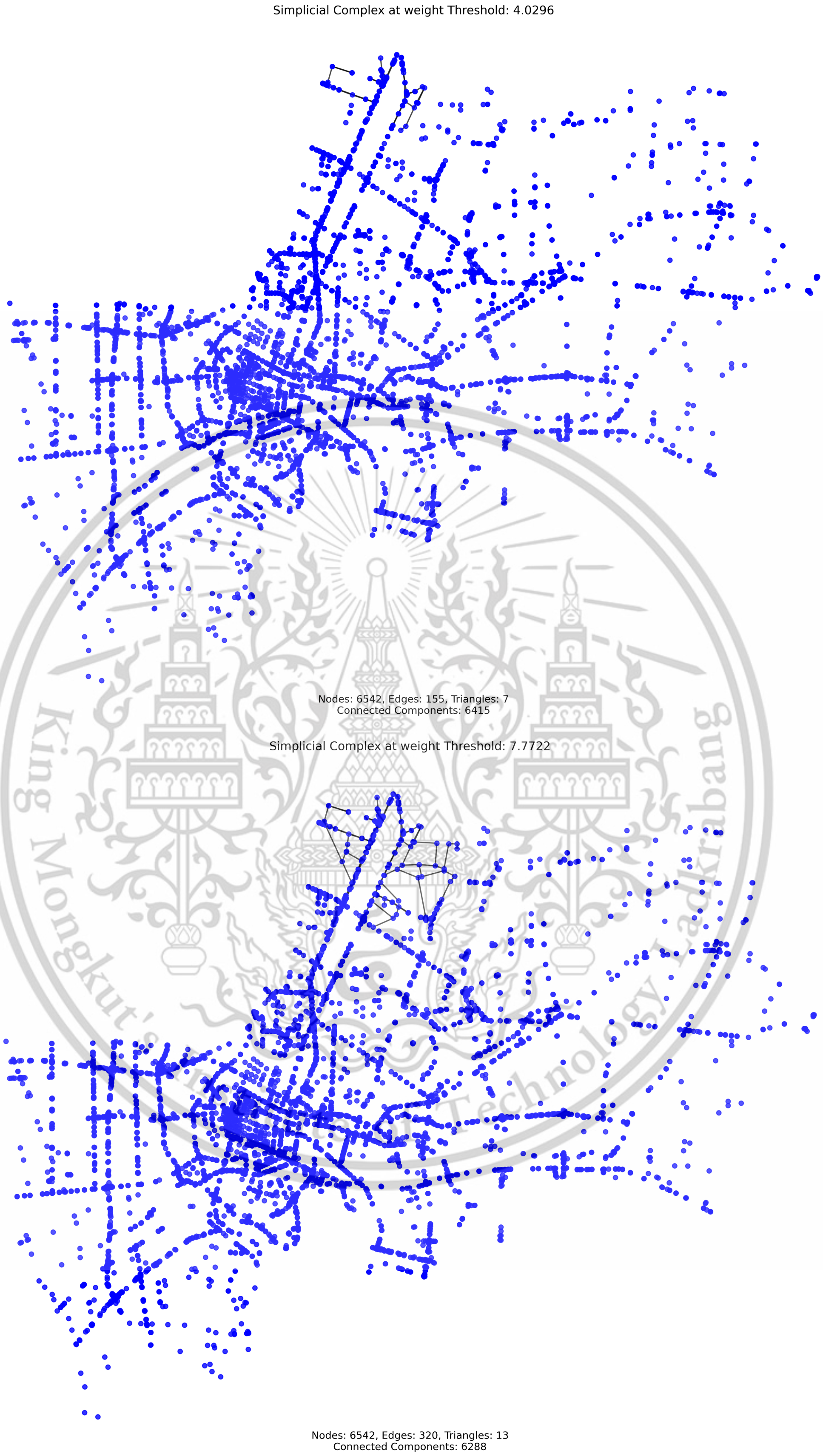

Figure 4.13 Visualization of the simplicial complex representing the Bangkok road network at four thresholds for the `reweighted_distance` parameter which are `reweighted_distance` $= 4.0296$ and 7.7722, respectively, selected using the evenly spaced strategy across the parameter range.

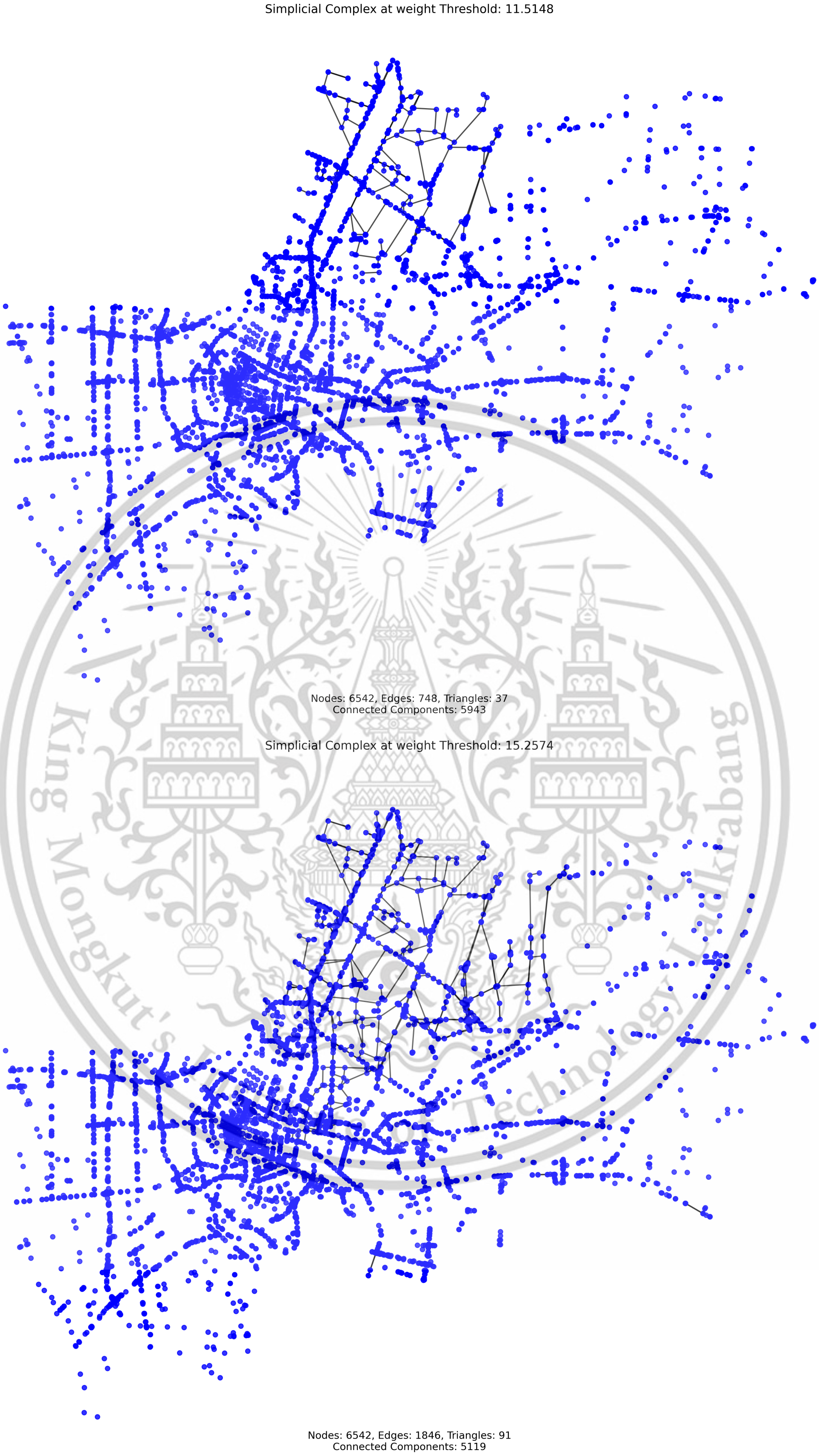

Figure 4.14 Visualization of the simplicial complex representing the Bangkok road network at four thresholds for the **reweighted_distance** parameter which are **reweighted_distance** $= 11.5148$ and 15.2574, respectively, selected using the evenly spaced strategy across the parameter range.

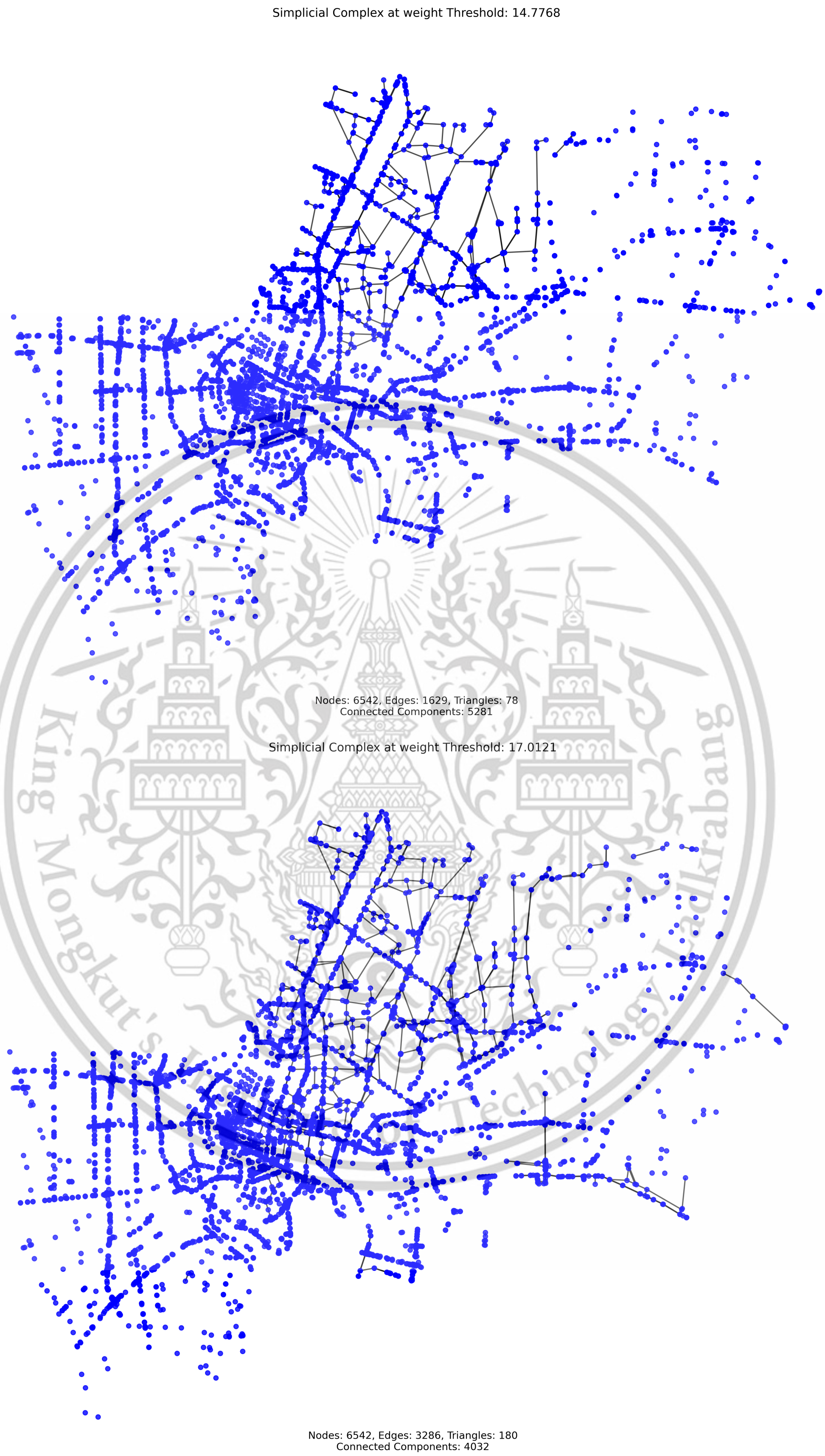

Figure 4.15 Visualization of the simplicial complex representing the Bangkok road network at four thresholds for the **`reweighted_distance`** parameter which are **`reweighted_distance`** = 14.7768 and 17.0121, respectively, selected using the persistence-based strategy across the parameter range.

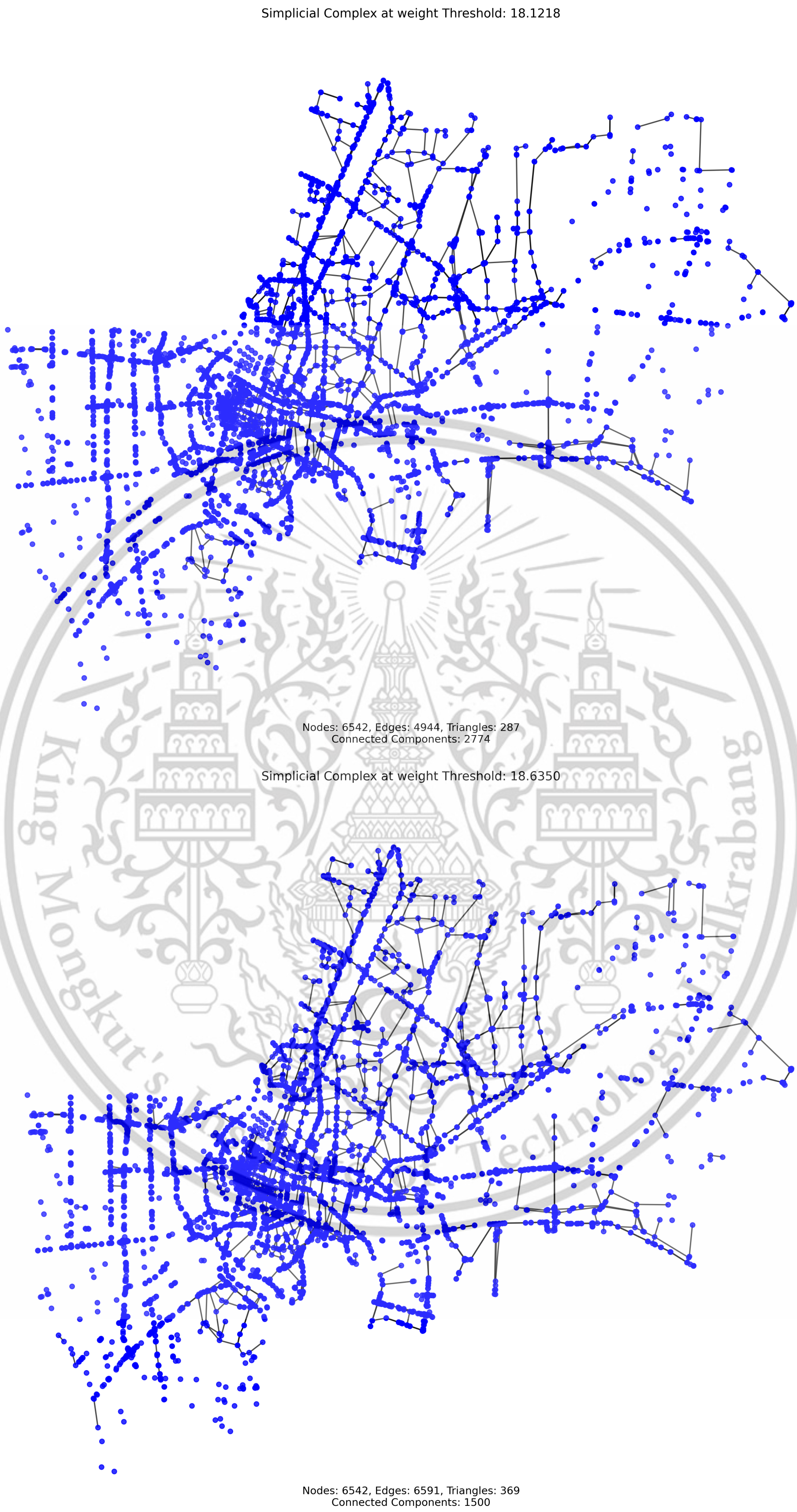

Figure 4.16 Visualization of the simplicial complex representing the Bangkok road network at four thresholds for the `reweighted_distance` parameter which are `reweighted_distance` = 18.1218 and 18.6350, respectively, selected using the persistence-based strategy across the parameter range.

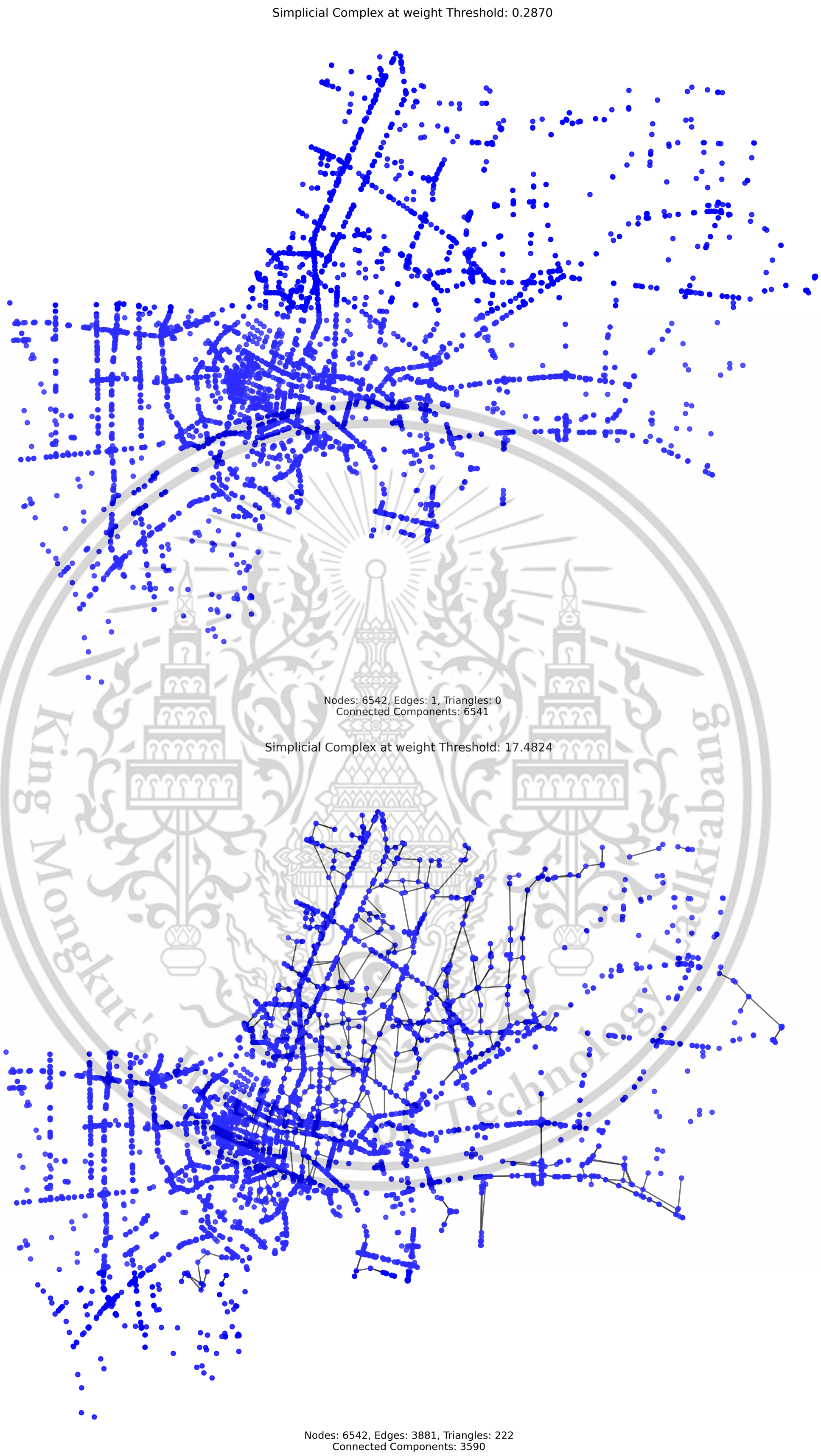

Figure 4.17 Visualization of the simplicial complex representing the Bangkok road network at four thresholds for the `reweighted_distance` parameter which are `reweighted_distance` = 0.2870 and 17.4824, respectively, selected using the component-based strategy across the parameter range.

Figure 4.18 Visualization of the simplicial complex representing the Bangkok road network at four thresholds for the `reweighted_distance` parameter which are `reweighted_distance` = 18.7029 and 18.8988, respectively, selected using the component-based strategy across the parameter range.

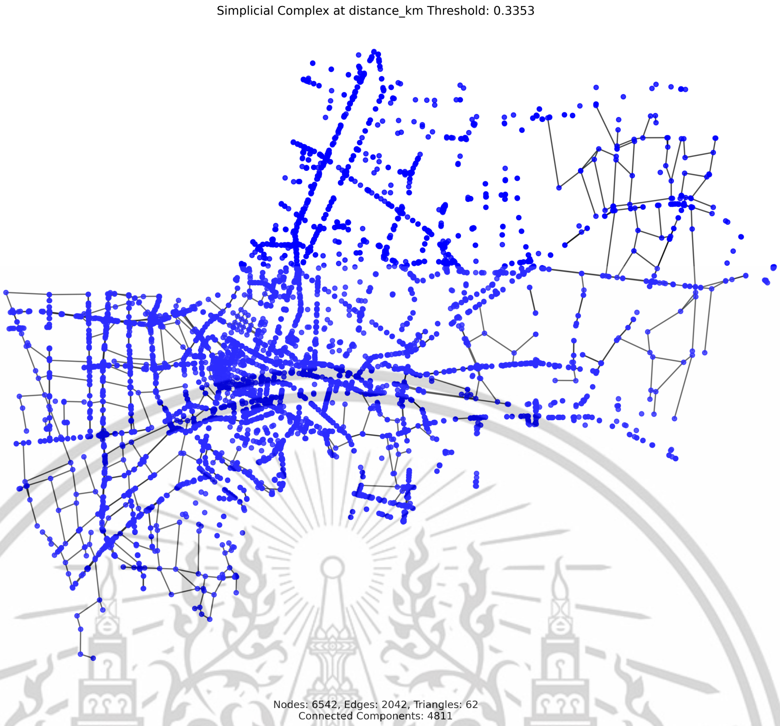

Figure 4.19 Visualization of roads that appear at `distance_km` = 0.3353

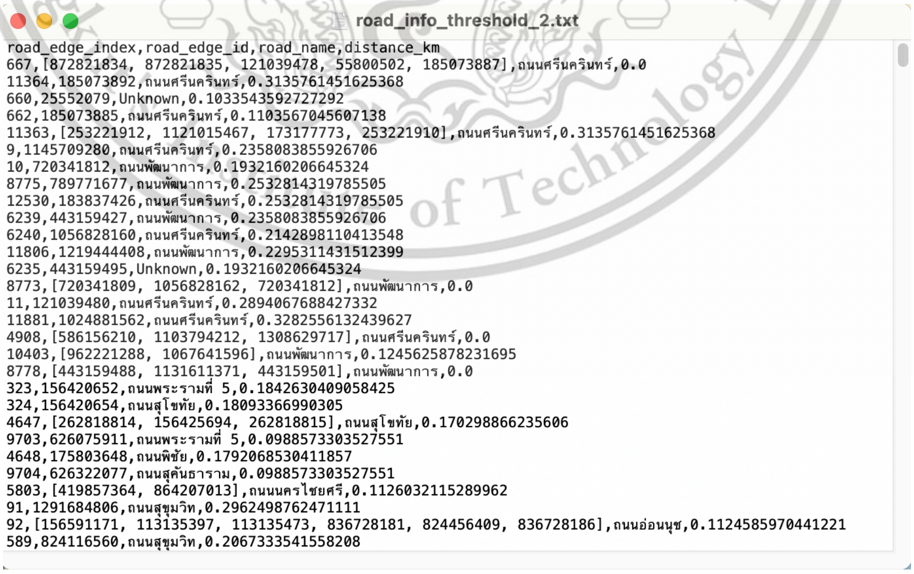

road_info_threshold_2.txt

```
road_edge_index,road_edge_id,road_name,distance_km
667,[872821834, 872821835, 121039478, 55800502, 185073887],ถนนศรีนครินทร์,0.0
11364,185073892,ถนนศรีนครินทร์,0.3135761451625368
660,25552079,Unknown,0.1033543592727292
662,185073885,ถนนศรีนครินทร์,0.1103567045607138
11363,[253221912, 1121015467, 173177773, 253221910],ถนนศรีนครินทร์,0.3135761451625368
9,1145709280,ถนนศรีนครินทร์,0.2358083855926706
10,720341812,ถนนพัฒนาการ,0.1932160206645324
8775,789771677,ถนนพัฒนาการ,0.2532814319785505
12530,183837426,ถนนศรีนครินทร์,0.2532814319785505
6239,443159427,ถนนพัฒนาการ,0.2358083855926706
6240,1056828160,ถนนศรีนครินทร์,0.2142898110413548
11806,1219444408,ถนนพัฒนาการ,0.2295311431512399
6235,443159495,Unknown,0.1932160206645324
8773,[720341809, 1056828162, 720341812],ถนนพัฒนาการ,0.0
11,121039480,ถนนศรีนครินทร์,0.2894067688427332
11881,1024881562,ถนนศรีนครินทร์,0.3282556132439627
4908,[586156210, 1103794212, 1308629717],ถนนศรีนครินทร์,0.0
10403,[962221288, 1067641596],ถนนพัฒนาการ,0.1245625878231695
8778,[443159488, 1131611371, 443159501],ถนนพัฒนาการ,0.0
323,156420652,ถนนพระรามที่ 5,0.1842630409058425
324,156420654,ถนนสุโขทัย,0.18093366990305
4647,[262818814, 156425694, 262818815],ถนนสุโขทัย,0.170298866235606
9703,626075911,ถนนพระรามที่ 5,0.0988573303527551
4648,175803648,ถนนพิชัย,0.1792068530411857
9704,626322077,ถนนสุคันธาราม,0.0988573303527551
5803,[419857364, 864207013],ถนนนครไชยศรี,0.1126032115289962
91,1291684806,ถนนสุขุมวิท,0.2962498762471111
92,[156591171, 113135397, 113135473, 836728181, 824456409, 836728186],ถนนอ่อนนุช,0.1124585970441221
589,824116560,ถนนสุขุมวิท,0.2067333541558208
```

Figure 4.20 An example of road segments identified at `distance_km` = 0.3353.

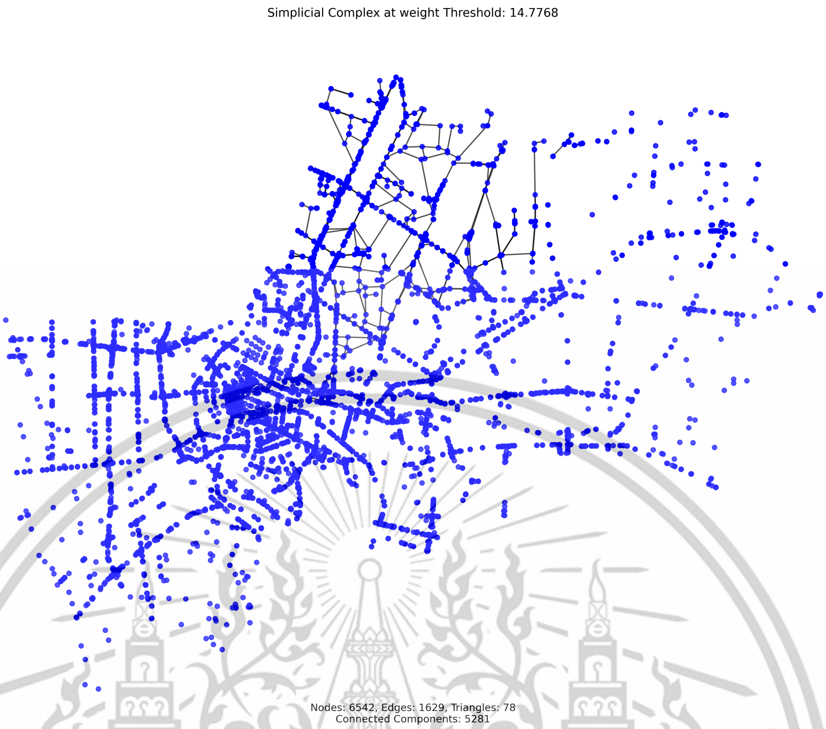

Figure 4.21 Visualization of roads that appear at `reweighted_distance` = 14.7768


road_info_threshold_2.txt

```
road_edge_index,road_edge_id,road_name,weight
7336,684512040,ถนนลาซาล,14.468380308845468
463,[1192571490, 998352540, 998352143],ถนนสุขุมวิท,14.455736377803628
1,[1192571140, 684512039],ถนนสุขุมวิท,14.468380308845468
462,998352142,ถนนแบริ่ง,14.175911047136116
16,468353997,ถนนอโศก-ดินแดง,14.300796489195058
17,468353999,ถนนเพชรบุรี,14.3089681312111
4953,453939262,ถนนเพชรบุรี,14.291281943661764
8144,1024852980,ถนนอโศก-ดินแดง,14.291281943661764
8145,468354000,ถนนเพชรบุรี,14.300796489195058
8146,1103794214,ถนนอโศกมนตรี,14.313433983625655
8959,1103794215,ถนนเพชรบุรี,14.319746526175006
10153,957714393,ถนนเพชรบุรี,14.50282927087872
8143,[1029189124, 342772453],Unknown,14.3089681312111
6071,156763643,ถนนเทียมร่วมมิตร,13.971939620944056
19,1059339511,ถนนรัชดาภิเษก,13.905839124448416
12323,[1314824672, 969940060, 1103847159],ถนนรัชดาภิเษก,13.908813979261858
6070,25775953,ถนนเทียมร่วมมิตร,13.919496376832708
4813,156763608,ถนนรัชดาภิเษก,13.919496376832708
6072,1156851243,ถนนรัชดาภิเษก,13.927825622061215
4811,[369892577, 156763618, 369892574, 156763622],ถนนรัชดาภิเษก,13.895505584674986
4840,377358387,ถนนสุทธิสารวินิจฉัย,14.26145323454454
4839,876391535,ถนนรัชดาภิเษก,14.299695414206088
4801,[876391536, 974520474],ถนนรัชดาภิเษก,14.26145323454454
4841,[942823785, 369388491, 369388492, 157053117],ถนนสุทธิสารวินิจฉัย,14.236309799895771
4806,1155963907,ถนนรัชดาภิเษก,14.24201909753756
4805,156763634,Unknown,14.265472646993238
30,156126121,ซอยสุขุมวิท 3,14.525914997942111
8865,453692575,ถนนเพชรบุรี,14.525914997942111
8868,453692981,ถนนเพชรบุรี,14.56989302829204
```

Figure 4.22 An example of road segments identified at `reweighted_distance` $= 14.7768$.

Chapter 5

Conclusion

Effective flood management strategies in Bangkok require a comprehensive understanding of the road network's vulnerability to flooding, particularly in relation to the city's extensive and complex waterway system. A thorough assessment of how road systems are impacted by their spatial proximity to these rivers and canals is fundamental to the development of robust urban planning programs and adaptive civic protection measures. This study aimed to investigate the topological structure of Bangkok's road network in relation to its extensive waterway system, employing persistent homology as the primary analytical tool. The central goal was to explore how insights derived from the network's evolving connectivity, based on proximity to waterways, could potentially inform flood management strategies within the urban context.

To achieve this, road network and waterway data for Bangkok were sourced from OpenStreetMap (OSM). A key step involved calculating the distance from each road segment to its nearest waterway. This distance metric served as a foundational parameter, interpreted as a proxy for flood proneness, and was used to construct graph filtrations in two distinct ways for persistent homology (H_0) analysis: first, using the direct distance (`distance_km`), and second, using an inversely related measure (`reweighted_distance`). The results of these persistent homology computations were systematically visualized using standard tools, including persistence barcodes, persistence diagrams, and plots of the zeroth Betti number (β_0) against the respective filtration parameter. Furthermore, the structural evolution of the network's simplicial complex representation was examined through visualizations at specific thresholds selected via evenly spaced, persistence-based, and component-based strategies.

The analysis revealed distinct topological behaviors under the two filtration schemes. The `distance_km` filtration highlighted rapid merging of connected components at low distance thresholds, indicating significant connectivity changes among roads situated close to waterways. Conversely, the `reweighted_distance` filtration showed accelerated component merging primarily at higher parameter values, corresponding topologically to the incorporation of roads closer to waterways into the network structure. Both analyses allowed for the identification of specific threshold values associated with significant topological transitions.

The discussion explored the potential applications derived from these findings. The `distance_km` analysis was presented as a potential tool for *Flood Risk Identification*, where components appearing or merging at low distance thresholds might indicate road networks potentially vulnerable to simultaneous flooding. The `reweighted_distance` analysis was discussed in the context of identifying potentially safer or more resilient routes, corresponding to components that persist under conditions representing greater distance from waterways. Finally, it was proposed that significant thresholds identified through persistent homology—marking values where the network's connectivity undergoes fundamental shifts (e.g., major component merging events)—could serve as data-informed candidates for establishing critical Flood Trigger Levels for escalating response plans.

Although this study used spatial proximity to waterways as the primary parameter for its topological analysis, the resulting identification of areas with high flood susceptibility demonstrates notable consistency with official flood-related data from Thailand's open government data portal; see [4] (specifically, dataset IGD-22, which includes information such as flood risk zones or historical flood extents). This alignment, itself a key method for initial assessment, shows that a focused topological analysis of waterway proximity effectively identifies areas aligning with known flood risks, offering vital early information for flood management.

However, it is crucial to acknowledge that this work serves as a preliminary investigation. The primary limitation lies in using distance to waterways as the sole parameter proxying flood risk. A comprehensive and accurate prediction or assessment necessitates the integration of multiple parameters directly related to flooding, such as precise road elevation relative to waterways, drainage capacity, rainfall intensity, and land use characteristics, see Mosavi et al. 2018, Rahmati et al. 2015, Tehrany et al. 2014 and Zhao et al. 2018. Furthermore, this analysis was restricted to H_0, focusing exclusively on connected components.

Therefore, future research should prioritize the development of multi-parameter weighting schemes or filtration functions that incorporate a richer set of flood-related variables. Extending the topological analysis to higher homology dimensions, particularly investigating H_1 (which represents loops or cycles), could yield valuable insights into network redundancy, potential bottlenecks, or areas prone to isolation during flood events.

In conclusion, this study should be viewed as a preliminary exploration into the application of persistent homology, using distance to waterways as a key parameter, for generating insights relevant to flood management in Bangkok. We emphasize that the methodology presented here is intended as a potential *decision-support tool*, rather than a direct flood prediction model. A primary contribution of this topological approach lies in its ability to analyze network connectivity; instead of focusing solely on individual road segments, it identifies and tracks connected components of roads that share similar characteristics related to water proximity—highlighting potential networks of high-risk or relatively resilient routes. This network-centric perspective provides valuable structural information that complements traditional flood susceptibility analyses, which often delineate high-risk areas but may not fully capture the critical connectivity patterns or potential isolation of road segments within those zones. By focusing on connected structures, this approach offers a different lens through which to assess vulnerability and plan interventions.

Bibliography

[1] Aktas, M.E., Akbas, E. and Fatmaoui, A.E. Persistence homology of networks: methods and applications. *Appl Netw Sci 4*, 61 (2019). https://doi.org/10.1007/s41109-019-0179-3

[2] Corcoran, P. and Jones, C. B. Topological data analysis for geographical information science using persistent homology. *International Journal of Geographical Information Science*, 37(3), 712–745.(2023) https://doi.org/10.1080/13658816.2022.2155654

[3] D. C. Mason, I. J. Davenport, J. C. Neal, G. J. . -P. Schumann and P. D. Bates, Near Real-Time Flood Detection in Urban and Rural Areas Using High-Resolution Synthetic Aperture Radar Images, *in IEEE Transactions on Geoscience and Remote Sensing*, vol. 50, no. 8, pp. 3041-3052. (2012) doi: 10.1109/TGRS.2011.2178030.

[4] Digital Government Development Agency (2022). Integrated Geospatial Data for Disaster Management Phase II. https:// data.go.th/dataset/igd-22

[5] Fernandez, D.S. and Lutz, M.A. Urban Flood Hazard Zoning in Tucumán Province, Argentina, Using GIS and Multicriteria Decision Analysis. *Engineering Geology*, 111, 90-98. (2010) http://dx.doi.org/10.1016/j.enggeo.2009.12.006

[6] Hatcher, A. *Algebraic topology*. Cambridge: Cambridge University Press. (2002) ISBN: 0-521-79160-X; 0-521-79540-0

[7] Herbert, E. A *Short Course in Computational Geometry and Topology*. Springer Publishing Company, Incorporated. (2014)

[8] Horritt, M.S. and Bates, P.D. Evaluation of 1D and 2D Numerical Models for Predicting River Flood Inundation. Journal of Hydrology, 268, 87-99. (2002) https://doi.org/10.1016/S0022-1694(02)00121-X

[9] J. Teng, A.J. Jakeman, J. Vaze, B.F.W. Croke, D. Dutta and S. Kim, Flood inundation modelling: A review of methods, recent advances and uncertainty analysis, *Environmental Modelling and Software*, 90, 201-216. (2017) https://doi.org/10.1016/j.envsoft.2017.01.006.

[10] Kundzewicz, Z. W., Kanae, S., Seneviratne, S. I., Handmer, J., Nicholls, N., Peduzzi, P. and Sherstyukov, B. Flood risk and climate change:

global and regional perspectives. *Hydrological Sciences Journal*, 59(1), 1–28. (2013) https://doi.org/10.1080/02626667.2013.857411

[11] Mosavi, A., Ozturk, P. and Chau, K-w. Flood Prediction Using Machine Learning Models: Literature Review. *Water*. 2018; 10(11):1536. https://doi.org/10.3390/w10111536

[12] Munkres, J.R. and Munkres, J.R. *Elements Of Algebraic Topology*. CRC Press. (1984) https://doi.org/10.1201/9780429493911

[13] Nair, S. , Wen, W. K. and Ling, C. M. Bangkok Flood Risk Management: Application of Foresight Methodology for Scenario and Policy Development. *Journal of Futures Studies*, 19, 87-112. (2014)

[14] Rahmati, O., Zeinivand, H. and Besharat, M. Flood hazard zoning in Yasooj region, Iran, using GIS and multi-criteria decision analysis. Geomatics, Natural Hazards and Risk, 7(3), 1000–1017. (2015) https://doi.org/10.1080/19475705.2015.1045043

[15] Schumann, G. and Alessio, D. Exploiting the proliferation of current and future satellite observations of rivers. *Hydrological Processes* 30, 2891 - 2896. (2016)

[16] Suthakaran, S., Withanage, A., Gunawardhane, M., and Gunatilake, J. A flood risk assessment based on an OpenStreetMap application: a case study in Manmunai North Divisional Secretariat of Batticaloa, Sri Lanka. *Bhumi, the Planning Research Journal*, 7(2), 23-30 (2020). https://doi.org/10.4038/bhumi.v7i2.46

[17] Tehrany, M. S., Pradhan B., Jebur, M. N., Flood susceptibility mapping using a novel ensemble weights-of-evidence and support vector machine models in GIS, *Journal of Hydrology*, 512, 332-343. (2014) https://doi.org/10.1016/j.jhydrol.2014.03.008.

[18] Wei X, Wei G-W. Persistent Topological Laplacians—A Survey. *Mathematics*, 13(2), 208. (2025) https://doi.org/10.3390/math13020208

[19] Zhao G., Pang B., Xu Z., Yue J. and Tu T., Mapping flood susceptibility in mountainous areas on a national scale in China, *Science of The Total Environment*, 615, 1133-1142 (2018) https://doi.org/10.1016/j.scitotenv.2017.10.037.

Biography

Name	Nalinpat Ponoi
Date of Birth	29 March 1996
E-mail Address	nalinpat.pn@gmail.com
Education	Bachelor of Science in Mathematics, Department of Mathematics and Statistics, Prince of Songkla University, Thailand (2018)